Fermi National Accelerator Laboratory

TM-963

Design for a New Wide-Band Neutral Beam for the Tevatron

J. Butler, J. P. Cumalat, P. H. Garbincius, J. Hawkins, and K. C. Stanfield
Fermi National Accelerator Laboratory
P.O. Box 500, Batavia, Illinois

April 1980
(Updated April 25, 1989)

Operated by Universities Research Association, Inc., under contract with the United States Department of Energy

Fermilab

TM - 963
6020.000

Design for A New Wide-Band Neutral Beam for the Tevatron

J. Butler, J. P. Cumalat, P. H. Garbincius,
J. Hawkins, and K. C. Stanfield
Fermilab

April, 1980

Abstract

Fermilab's two photon beams, the tagged beam and the broad-band beam, do not run simultaneously because they must share the same primary proton beam and some beam enclosures. We demonstrate that the present broad-band beam is inadequate for operation at 1 TeV and propose to replace it with a versatile Wide Band Charged and Neutral beam. We discuss the necessary improvements to Proton East primary beam transport systems, the new beam optics and acceptances, the targeting scheme, expected fluxes, backgrounds from muons, and unwanted hadrons in the beam, the radiator and dump areas, the required experimental hall and its facilities, and a possible time table.

Addendum to TM-963

P.H. Garbincius 25 April 89 (rev. 31 May 89)

A. TM-1552: Wide Band to "Double Band" Upgrade, P. Kasper, et al., describes the 1989 beamline upgrade to increase the photon flux by transporting both electrons and positrons simultaneously.

B. As built instrumentation drawings are available from the Research Division Electrical/Electronics Department for this beamline. Reference numbers are:

2430-ME-172105-10
-17
-18
-19

C. The electron flux integrated over the full beam line acceptance per incident 800 GeV proton was measured in 1985 and is shown in the following figure. The typical momentum bite is sigma (dp/p) = +- 13 %. The fitted parametrization is:

$$\text{Electron Yield per Incident Proton} = A\,(1 - x)^{n}$$

where x = electron momentum/proton momentum

$A = 9.3 \times 10^{-4}$ and $n = 5.39$

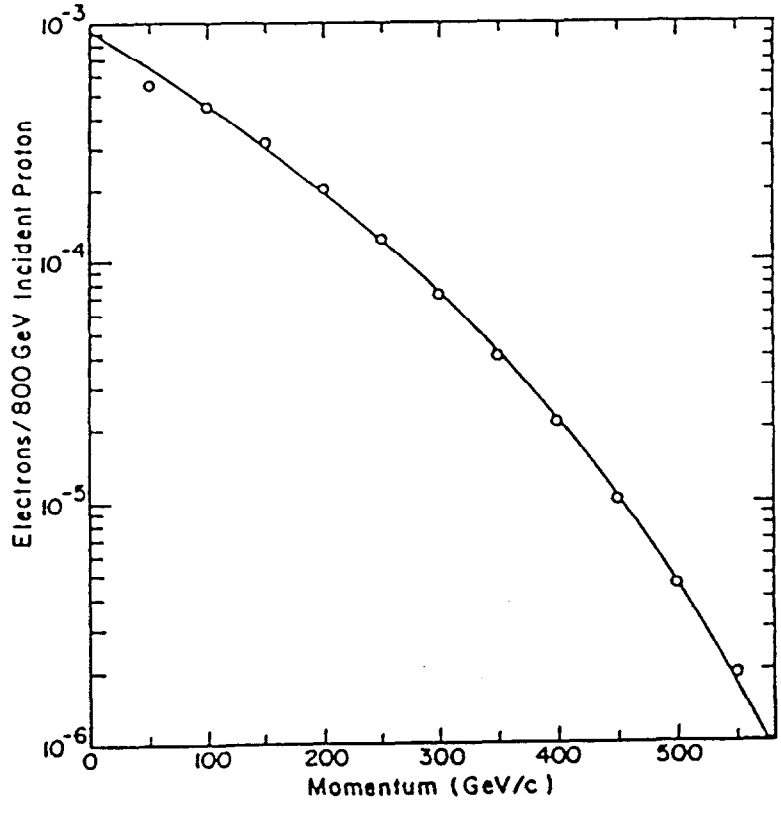

TABLE OF CONTENTS

I. Introduction

Proton East is one of three separate primary proton beam target areas in the Proton Laboratory. An overview of the Proton Area showing the relationship of Proton East to the other beam lines is indicated in Fig. 1. The existing primary beam target system in Proton East is capable of targeting beams as intense as 6×10^{12} 400 GeV protons in a 1 sec slow spill with a 10 sec cycle time. This capability has been used to perform a variety of experiments which include the precision single arm, high $P_\perp$ measurements of the Chicago-Princeton group.[1] However, most of the emphasis in this area has been on experiments with beams of photons. Two secondary beams, the Tagged Photon Beam[2] and the Broad Band Beam,[3] share the P-East primary proton beam and target system. For this reason only one of these beams can be operated at any given time. In spite of this inefficiency, the results of experiments in Proton East have contributed importantly to our knowledge of high energy interactions.

Several experiments have reported results on high-energy photoproduction of vector mesons.[4] One of these demonstrated that the ψ is a hadron.[5] The total cross section for a photon to produce hadronic final states was measured up to 200 GeV.[6] This result indicates that the level of charm production in photon interactions is on the order of 1 μb. Photoproduction of $\bar{\Lambda}_c$, D* and D^0 has been measured.[7] In addition, the neutron experiment in P-East made the first measurement of ψ hadroproduction at Fermilab energies.[8] The same experiment ruled out the reaction $n + N \to \psi + c\bar{c} + X$ as the primary mechanism for producing charm in hadron collisions.[9]

Limitations of Existing Beam

The Broad Band Beam, located in Proton East, is the most intense source of high-energy (>100 GeV) photons presently available at any accelerator. For several reasons, this beam is now reaching the end of its usefulness and should be replaced by a different kind of beam. These reasons are:

(i) The beam contains a significant background of neutral hadrons (neutrons and K^0_L's). For a typical experiment triggering on hadronic final states, experience has shown that the number of events induced by the interactions of hadrons is approximately equal to those induced by photons. The problem is exacerbated at the highest energies where the contamination from neutrons is greatest. Experiments using the beam have been limited to $x \lesssim 0.5$ (or 200 GeV for 400 GeV incident protons) because of neutron and K^0_L contamination.

(ii) It is not possible to use the Broad Band Beam and the Electron Beam simultaneously. Access to the Broad Band detector building is prohibited because of radiation from Electron Beam elements while the Electron Beam is running. This has resulted in very inefficient use of beam time in Proton East and discourages the installation of a major new detector in the existing enclosure.

(iii) Muon rates in the detector building are unpleasantly large. Extrapolation of experience at 350 GeV, 400 GeV and 450 GeV indicates instantaneous muon fluxes in EE4 of $\sim 2 \times 10^7/\text{sec}/\text{m}^2$ for 6×10^{12} protons at 1 TeV in a 20-second spill.

(iv) The Broad Band Beam and the Electron Beam share the same target box. This necessitates frequent changeovers involving relocation of pre-target beam elements, resulting in unnecessary radiation exposures, operating costs, and loss of beam time.

Design Goals

A new beam, whose primary purpose is to replace the existing Broad Band Beam, should, above all, be an intense source of high-energy photons. Our criteria are: The photon flux should be at least an order of magnitude more intense than the existing Tagged Photon Beam flux at all energies. The photon beam should be as free as possible of hadron contamination and at least an order of magnitude better than the existing Broad Band Beam. The muon background in the experimental hall should be sufficiently small so that singles rates in detectors are dominated by other sources (i.e., e^+e^- pairs). In addition, experiments using muon (di-muon) triggers should be possible using the maximum achievable photon flux.

If possible, the beam should be a flexible source of hadrons as well as photons. The existing beam (Broad Band Beam) is also a neutron and K^0_L beam. Ideally, this capability should be maintained.

Finally, the experimental hall for the new beam should be designed with adequate facilities for the support of two major detectors for 1 TeV experiments.

Design Solution

The solution chosen to accomplish these goals is:

(i) The existing Broad Band Beam will be replaced by a new high energy, high intensity electron beam. The new beam will

have very large momentum acceptance, ± 15%, and large solid angle ∿ 4 μ ster. It will be able to transport electrons up to 800 GeV. These will be converted to photons in a radiator. The beam will be operated as a bremsstrahlung beam with no tagging of the photon energy. In this manner, high fluxes of photons up to 500 GeV can be obtained. We estimate that the hadron background will be reduced by at least an order of magnitude from that of the existing Broad Band Beam. We also intend to maintain the capability of having a high energy neutral beam. This is accomplished by having zero net deviation from the direction of the incident proton beam. A similar beam has been proposed and built for lower energy operation at CERN.[10]

(ii) A splitting station will be installed in Proton East so that two beams can be targeted simultaneously.

(iii) A new detector enclosure will be constructed for the new beam approximately five hundred feet farther from the target point than the present detector building. This will provide additional space and flexibility for muon shielding.

(iv) The new beam will be targeted in a new location far downstream of the present target box, which will continue to serve the Electron Beam.

Beam Design

An overview of the new beam, its target box, and detector building is given in Fig. 2 and 3. The primary proton beam is transported through the present target box and is bent 30 mrad to the east by four Energy Saver dipoles. A system of Energy Saver

quadrupoles located in EE1 focuses the proton beam on a production target at the upstream end of EE4, the present Broad Band Beam experimental detector enclosure. The target box is followed immediately by a flux gathering quadrupole lens and dipoles that disperse the beam in momentum. An enclosure (dipole enclosure) contains a dump for neutral particles, a momentum collimator, and additional dipoles that begin to recombine the beam. The final stage completes the recombination of the beam and produces a focus at the experimental target. The radiator and appropriate sweeping magnets are located in this area. There is sufficient space in the new experimental hall to support two experiments.

Because the net deflection of the dipoles in the beam is zero, it is possible to make a neutral beam by removing the neutral beam dump in the dipole enclosure. The target box magnet will be energized sufficiently to dump all charged particles produced at the primary target inside the shielded target box. The beam line magnets may serve as downstream sweeping elements. Another attractive feature of the beam is that a primary proton beam could be made available in the experimental hall by turning off the target box magnet.

II. Secondary Beam Optics and Acceptances

This high-flux beam is designed to transport a large-momentum bite (±15%) charged particle beam from the production target located in EE4 to an achromatic x, y focus in the new experimental hall. The tunable range of this charged particle channel is 400-800 GeV/c. The beam spot is 2.5 x 1.5 cm with divergences of $\delta\theta_x$ = ±0.6 mrad, $\delta\theta_y$ = ±0.5 mrad. The acceptance is computed by a Monte Carlo program to be 120μster-%. A complete list of beam elements is given in Table I. The optical properties are summarized in Table II.

The design criteria discussed earlier require that we maintain the possibility of a zero-degree neutral beam. Therefore, the secondary beam is brought back to the same line as the incident proton beam by a double dog-leg bend with zero net deflection. The design philosophy is to minimize geometric and chromatic aberrations by keeping the first order structure of the beam symmetric about the midpoint of the beam line (Fig. 4) so that sextupole correction elements are not necessary.

The length of the beam was chosen to be 1000' to reduce the muon halo background in the experimental hall (see Sec. V). The choice of magnetic elements was limited in this design exercise to conventional magnets with 4"-6" apertures and maximum pole-tip fields of 20 kg for dipoles and 12 kg for quadrupoles. Further studies, later, may show that improvements over the present design are possible by replacing selected beam elements with larger bore superconducting magnets. We do not intend to rule out such possibilities. This particular design should be regarded as an existence proof of what acceptance may be obtained with existing Fermilab beam elements. Finally, limiting apertures must be located far upstream so as to minimize beam halo.

This beam line will have two different optical configurations for transporting charged particles, a broad band mode and a narrow band mode. When the beam is tuned for large momentum acceptance the lowest momentum ray, P_L, that is within the accepted momentum bite is transported through two optical stages. The first stage has point-to-point imaging between the production target and the momentum slit. The second stage has point-to-point imaging between the momentum slit and the experimental target and produces an achromatic x, y focus at that point. The highest momentum ray, P_H, within the acceptance is transported as though the beam had only one optical stage with point-to-parallel-to-point imaging between the production target and the experimental target. Fig. 5 illustrates some first-order imaging properties of rays P_L and P_H for the broad band tune. The narrow band mode is achieved by selecting a smaller momentum bite using the momentum slit. In this mode, the beam is operated as a standard two-stage transport with point-to-point optics in each stage.

The bend angle is determined by the desired momentum dispersion and the amount of bending necessary to separate cleanly the neutral beam from the e^- beam and maintain the first order optical symmetries as described above. The double dog-leg configuration of dipoles between two quadrupole triplets produces a momentum-dispersed beam after the first triplet and recombines the beam before the beginning of the second triplet. Since there is no first-order dispersion within any of the quadrupoles, a large momentum acceptance is achieved.

III. Splitting Station, Targeting Scheme, Target Box, Neutral Dump and Momentum Slit

In order to achieve the design objectives described in Section I, we propose a new targeting scheme which allows this beam to run simultaneously with the Tagged Photon Beam and is flexible enough to permit operation in several different modes. It is possible to obtain electron/photon, π^-, neutron, K^0_L, and primary proton beams. Details of the targeting and beam dumps required for all these different beams are discussed in this section.

Beam-Splitting Station

We have emphasized the importance of being able to provide beams simultaneously to both the Tagged-Photon Lab and the Wide Band Beam Lab. The first step in this process is to split the primary beam in Proton East into two separate beams. This is done by directing the east branch of the primary beam onto four electrostatic septa located at the downstream end of the upgraded version of Enclosure H[11] Each septum is 3.1 m long with a gap of 20 mm and can be operated at voltages up to 70 KV. A trim dipole magnet located 115' upstream steers the beam onto the septa and may be used to adjust the split ratio. The four septa deflect the protons above the wires up through an angle of .044 mrad and those below down through an angle of .044 mrad. These two slightly-divergent beams drift 1000' in the existing 12" vacuum pipe from Enclosure H to a new pit, Enclosure K, which contains three standard 2-way Lambertson magnets that separate the beams horizontally. The vertical separation of the two beams at the Lambertsons

is 1". The beam for the Tagged Photon line is undeflected while the beam for the Wide Band line is bent to the east through an angle of 2.1 mrad. The beams leave Enclosure K in the same 12" vacuum pipe and travel about 300 feet. The beams are separated horizontally by 8". At this point there is a transition piece and the two beams drift the remaining 700' to the P-East pre-target hall in separate vacuum pipes. The beam for Tagged Photon comes in along the same line as it does now. The new beam is displaced approximately 25" to the east, enough to clear the yokes of the Tagged Photon Beam pre-target elements. The new beam drifts through a vacant slot in the existing P-East target box and is then transported by its own pre-target magnet system described in the next section. Fig. 6 shows the layout of the Proton East beam components in Enclosure H. Fig. 7 shows Enclosure K and its elements. The elements involved in the split and some relevant parameters are summarized in Table III.

Pre-target Optics

The pre-target optics consists of 4 ED/S dipoles, a quadrupole doublet consisting of a total of one 3Q120 and 6 ED/S quadrupoles, and 3 main ring dipoles (B2's). This system accomplishes three objectives:

1) The 4 ED/S dipoles deflect the primary proton beam through an angle of 30 mrad to the east. This produces a very large separation between the Tagged Photon Lab and the Wide Band Beam Experimental Hall, and is necessary to decouple each beam from the other's muon background. For example, forward-going muons from the primary target and neutral dump of the Tagged Photon

Beam pass far to the west of the Wide Band Beam Experimental Hall.

2) The quadrupole doublet takes the approximately parallel incoming proton beam and focuses it onto a 1 mm x 1 mm production target in EE4. The 6 ED/S quadrupoles are operated both electrically and cryogenically in series. Because the two sections of the doublet actually need to have slightly different strengths, a 3Q120 precedes the cryogenic quadrupoles. Its current is adjusted to obtain a proper focus. Based on present experience, the beam entering this doublet will have a size of 20 mm x 20 mm and an angular divergence of $\pm$ 20 μradians. At the target, the spot size, which is proportional to angular divergence, will be $\pm$ 1 mm. At the primary proton dump the spot size will be $\pm$ 2 mm.

3) The system of 1 EPB dipole and 2 main ring dipoles (B2's) is used to vary the angle and position of the beam entering the target box. This system is discussed in detail below.

Fig. 8 and Table IV list these pre-target elements and give some relevant optical properties.

The cryogenic elements in the pre-target area will get their liquid helium from the satellite refrigerator which supplies the Electron Beam pre-target components. This refrigerator is located in the P2 service building.

Targeting Scheme

The targeting scheme proposed for this beam is schematically represented in Fig. 9. The pre-target bend geometry and target box magnets are arranged for use with both charged and neutral secondary beams. In addition, flexibility is maintained for

producing finite angle beams such as diffractive proton or polarized proton beams from polarized Λ^0 decays. All targeting bends are vertical, to prevent introducing muon backgrounds into the Tagged Photon Lab. The protons are dumped downward, and zero-degree production of the charged(neutral) beam is directed downward (level) to prevent a rising muon cone as exists in the P-East Electron Beam. The primary proton beam is level through EE1 and the secondary beam is also level, downstream of the target box. This will simplify construction and alignment, and minimize above-ground radiation problems.

The primary proton beam is pitched vertically by an EPB dipole at the downstream end of EE1. This may be replaced by a modified B1 dipole if horizontal aperture problems arise. Two B2 dipoles in the EE4 pre-target area will position the primary beam horizontally on the neutral beam production target, or at 5 mrad downward angle on the charged-beam target. The required currents are:

	Charged Beam	Neutral Beam
EPB	+1600 A	-1600 A
B2	-4500 A	+1200 A

The production target will be located just inside the first target box B2 dipole magnet. It will consist of a small-diameter Be wire, 18 inches long. This will be cooled by a gaseous Helium flow. The dumping system will consist of two B2 dipole magnets with internal hadron absorbers, and a water-cooled collimator/dump similar to that used in the present HIA beam line.[12] Two B2 magnets are necessary to dump the zero-degree primary protons cleanly 3/4 inch into the lip of the dump. The aluminum dump utilizes the good thermal conduction properties of aluminum, allowing the cooling water channels to be placed a few inches away from

the dump point. Brass or copper liners will fill the gap of the B2 magnets to absorb pions produced in the primary target before they have a chance to decay and produce muons. The 40 foot long x 4 inch wide bend field is also very effective in sweeping all decay muons transversely beyond practical detector dimensions in the downstream experimental hall. The standard B2 magnet is chosen for ready availability of replacements. Finally, a solid iron dipole magnet may be placed immediately downstream of the aluminum dump to help sweep away muons induced in the dump by pion decays or by prompt muons.

The secondary beam channel dimensions are limited to $\pm$ 0.75 mrad vertically by $\pm$ 1.00 mrad horizontally to shadow all downstream magnet apertures totally in order to minimize muon production by scraping of the zero-degree, high-energy neutron spectrum. Muon backgrounds will be more fully discussed in Section V.

Neutral Dump

In the electron beam mode, the flux of neutrons, K^0_L's and photons not converted by the lead converter must be dumped downstream. The dipole magnets at the end of EE4 bend the electron beam to the east by an angle of 3 mrad. At the entrance to the dipole enclosure, the electron beam is separated from the unwanted neutral flux by 9". The size of the neutral beam is determined by the aperture in the primary beam dump and is $\pm$ 3.6" vertically and $\pm$ 4.8" horizontally. The position of the electron beam, the neutral beam, and the neutral dump at the entrance to the dipole enclosure is shown in Fig. 10a.

We have chosen an aperture-defining collimator in the target box which keeps the neutral beam small enough so that it is transported cleanly to the dump without scraping on the upstream elements. In particular, the vertical angle bite is made slightly smaller than the horizontal angle bite so that the neutral beam can safely pass through the 3" vertical aperture of the first two bend magnets. Fig. 10b shows the size of the neutral beam both at the final quadrupole of the first stage and at the two dipoles immediately following it.

The flux of neutrons incident on the dump is 5×10^{10} per 10^{12} incident 1 TeV protons. The K^0_L flux is negligible by comparison. The photon flux is 5×10^{10} per 10^{12} protons and has lower average energy than the neutron flux. The power in this flux at the highest anticipated incident proton intensity is sufficiently low that it can be dumped in a simple steel plug which does not need to be water cooled. Preliminary studies, Section V, indicate that there will not be a significant contribution to the flux of muons in the experimental hall from this dump. If further calculation shows that this is in fact a problem, the dump may be magnetized and may be followed by additional magnets which will sweep the muons away from the hall.

Momentum Slit

The dipole enclosure also contains a variable aperture collimator which can be used to control the intensity. This collimator is located downstream of the neutral dump and just upstream of the set of 4 dipoles which begin to recombine the beam and bend it back to the zero-degree line. The collimator is located at the point where the lowest momentum accepted particles form a focus. At

the largest momentum bite, the high momentum particles within the acceptance are not well focused at this location. This means that the correlation between momentum and position at the collimator is not complete for wide momentum acceptance operation. Fig. 11 shows the relation between horizontal position and momentum for 700 GeV operation.

In the charged pion mode, the momentum collimator may intercept as much as a few 10^{10} negative pions and may contribute significantly to the muon rate in the experimental hall. If this is true, the collimator will be followed by spoilers or sweeping magnets to deflect the muons away from the experimental apparatus.

IV. Flux Calculations

In this section, we present the results of flux calculations for the proposed beam and compare the predictions to the fluxes of other existing and proposed beams. Rather than calculate for a fixed arrangement of components, we do the computation for a solid angle and momentum bite that is typical of the various beam optics that are being considered. We begin with a brief description of the computations and then present the predicted yields for π^-, e^-, γ, n, K^0_L and p.

Details of the Calculations

For calculation of pion, electron, and photon yields, one begins by generating a parent pion distribution according to some production model which describes the available data. Neutral pions are assumed to be produced with exactly the same distribution as π^-. We have chosen to use the Bourquin-Gaillard model.[13] In this model, the spectrum of produced pions is described by:

$$E\frac{d^3\sigma}{d^3p} = \frac{A}{(E_T + B)^C} f(y) \begin{cases} e^{-P_\perp} & ; P_\perp < 1 \text{ GeV/c} \\ e^{-D(P_\perp - 1)/\sqrt{s}} - 1 & ; P_\perp > 1 \text{ GeV/c} \end{cases}$$

where $f(y) = e^{-\alpha/y^\beta}$ and $y = \ln\left\{\frac{E_{max} + P_{e\,max}}{E + P_e}\right\}$.

B = 2 GeV, C = 12.3, D = 23 GeV, α = 5.13, β = 0.38

and A/σ_{tot} = 78.15.

Here P_L and P_t are the longitudinal (cm) and transverse momentum and $E_t = \sqrt{P_t^2 + m_\pi^2}$.

For neutron production, we use the experimental results on inclusive neutron production on Beryllium of Whalley et al[14] and the yields measured near 0^{o} in the Broad Band Beam at Fermilab. These show a triangular-shaped momentum spectrum peaking at $\sim 3/4$ of the primary beam energy.

$$\frac{d^2\sigma}{dp\,d\Omega} = \begin{cases} E_{inc}\, A\, \frac{x}{x_p}\, e^{-b p_\perp} & ;\ x < x_p \\ E_{inc}\, A \left[\frac{1-x}{1-x_p}\right] e^{-b p_\perp} & ;\ x \geq x_p . \end{cases}$$

Here x is the Feynman-x value, E_{inc} is the incident beam energy, x_p is the x-value at which the distribution peaks and p_t is the transverse momentum.

$$x_p = 0.75$$

$$b = 2.5\ \text{GeV}^{-1}$$

$$A = 24.2$$

For the calculation of the K^0_L flux we use data on the forward production of K^0_S by protons.[15] The invariant cross section is parameterized as :

$$E\frac{d^3\sigma}{d^3p} = R(1-x)^F\left\{1 + d(1-x^4)\right\}$$

$$R = 5.6 \pm 0.8\ ,\ F = 3.4 \pm 0.2\ ,\ d = 0.8 \pm 0.7 .$$

For calculating the flux of elastically produced protons at angles corresponding to intermediate values of t ($t \sim 0.25\ \text{GeV}^2$), we use:

$$\frac{d\sigma}{d\Omega} = \begin{cases} 94.4 \frac{P^2}{\pi} e^{-12|t|} & ; |t| < .1 \\ (9.05 \times 10^6) e^{-10(|t|-.1)} & ; .1 < |t| < .5. \end{cases}$$

The slopes are taken from data at ISR.[16]

For the production target, we use 1.2 collision lengths of Beryllium. The reason for this choice is that the yield of photons does not increase for longer targets because the photons begin to convert before they leave. On the other hand, the relative yield of neutrons to photons leaving the target does increase as the target is lengthened. Fig. 12.a shows the photon yield vs. target thickness and Fig. 12.b shows the ratio of neutrons to photons vs. target thickness. In addition to being the optimum choice for the electron or photon mode of operation, 1.2 collision lengths of Beryllium is quite acceptable as a target in neutron, charged pion and diffractive proton modes.

The shape of the production target is 1 mm square. The pre-target optics discussed above is capable of focusing the entire extracted proton beam onto this target.

To form an electron beam, one inserts a converter downstream of the target to convert forward produced γ's into e^+ e^- pairs. The electrons then enter the magnetic channel to form the beam. In our calculations, we use 0.6 radiation lengths of lead as the converter. Fig. 13 shows that longer converters do not increase the number of electrons in the momentum region under consideration because of the increased probability that the electron will

bremsstrahlung before it leaves the converter. Longer converters increase the pion contamination in the beam through neutron interactions. The 0.6 radiation length lead converter corresponds to only 1½% of an interaction length.

The acceptance used in calculating π^-, e^-, and γ fluxes is:

$$\Delta\theta_x = \pm 1 \text{ mrad}$$
$$\Delta\theta_y = \pm 0.75 \text{ mrad}$$
$$\Delta p/p = \pm 15\%.$$

The acceptance is assumed to be uniform over these ranges of variables. This simplified view of the beam described in Section II is quite adequate for a flux calculation whose main purpose is to define the capabilities of the beam for doing physics.

Results

(i) Pion Yield

Fig. 14 shows the flux of pions produced with energies above 350 GeV as a function of vertical angle acceptance. There is little advantage to be gained from increasing the angular acceptance beyond $\pm$ 1 mrad. The sharp P_t cut off in hadronic collisions guarantees that 90% of all high energy pions fall within this acceptance. Fig. 15 gives the number of π^- per incident proton for a $\pm$ 15% momentum bite around several central momentum settings. Fluxes of pions typically used in open geometry experiments, about 10^8 pions/minute, can be obtained from modest numbers of primary protons ($\sim 10^{11}$/minute).

(ii) Electron Yield

Fig. 16 shows the electron yield in momentum intervals of $\pm$ 15% around various central momentum settings. The calculation includes the effect of photon conversions in the production target and bremsstrahlung of outgoing electrons in the converter.

(iii) Photon Yield

The photon yield is calculated from the electron flux based on a 30% radiator. Photon spectra for electron beam settings of 450 GeV and 600 GeV are shown in Fig. 17. The hadron background in this beam is discussed in a later section.

(iv) Neutron Yield

The acceptance of the 0^{o} neutron beam is limited by the physical apertures of the last few downstream elements. For the purposes of this calculation we assume a maximum spot size of 2" x 2" at a distance of 1000' from the production target. This corresponds to a solid angle of 28 nster. Table V shows the neutron yield for this acceptance and for two smaller acceptances, 10 nster and 2 nster (which are more typical of acceptances which have been used in actual experiments).

(v) K^{0}_{L} Yield

While the K^{0}_{L} yield is quite large, the number of K^{0}_{L} is only ~3% of the number of neutrons. To make a K^{0}_{L} beam of reasonable purity, one passes the neutral beam through an absorber which selectively removes the neutrons because of their larger interaction cross section. The K^{0}_{L} yield and

the neutron contamination for different conditions are shown in Fig. 18. It is possible to obtain a relatively pure sample of K^0_L induced events even for $n/K^0_L \sim 1$ since the total energy of K^0_L induced events is much lower than the energy of neutron induced events.

(vi) Proton Beam

A 1 TeV primary proton beam can be transported to the experimental hall by operating the beam as a single stage point-to-parallel-to-point transport. An alternative method of providing a 1 TeV proton beam is to form a diffractive beam. There are a variety of ways to do this, some of which involve dumping the primary beam downstream of the target box in the momentum collimator. The intensity is varied by changing the angle at which the primary beam strikes the production target. The yield of 1 TeV protons is shown as a function of targeting angle in Fig. 19. The angular acceptance assumed in this calculation is $\pm$ 1 mrad horizontal angle and $\pm$ 0.05 mrad about the various central vertical angles shown.

Flux Summary

Table VI summarizes the yields of particles in a manner that will be useful for thinking about the kinds of experiments that can be done with this beam. Fig. 17 compares the photon yields with the Tagged Photon Beam and the present Broad Band Beam and other similar beams. The pion yields are comparable to those expected in the P-West High Intensity Beam.[12]

V. Experimental Backgrounds

Two kinds of backgrounds make the present Broad Band Beam a difficult environment in which to do experiments. First, there is a large contamination of neutral hadrons in the photon beam. Second, there are large fluxes of muons in the vicinity of the detector which will increase substantially if the primary beam energy is raised to 1 TeV (see introduction). These backgrounds have caused problems with trigger rates, accidentals, counter dead-times and singles rates which have prevented experiments from using the high intensity that the beam is, in principal, capable of providing. In addition, the hadron contamination produces backgrounds which tend to obscure physics which would be quite clean in an intense photon beam of high purity.

Our objective in designing this new beam is to produce an environment in which these backgrounds are reduced by at least an order of magnitude. The next two sections discuss the reduction of hadronic contamination and muon backgrounds.

Hadronic Background

One of the most serious backgrounds to photoproduction experiments in the present version of the Broad Band Beam is the large contamination of neutral hadrons - K^0_L's and neutrons. Although only ½% of the particles in the beam are neutral hadrons, they account for approximately one-half of all hadronic final states that are produced. The advantage in signal-to-noise that photoproduction has over hadron production for certain kinds of final states, including those containing charm, is thus partially cancelled.

The new Wide Band Beam will have two orders of magnitude less hadron contamination. The hadronic background is due to neutrons interacting in the lead converter and producing negative pions which are

accepted by the electron beam transport. A small fraction of the negative pions then interact in the downstream radiator. A small fraction of these interactions produce forward-going neutral hadrons which can interact in the experimental targets. Calculations using data[13-15] on neutron and π^- production by protons have predicted a ratio π^-/e^- of 4% at the radiator. The radiator may be as thick as 30% of a radiation length corresponding to 1% of an absorption length. The ratio of interacting hadrons to photons will thus be less than 1.3×10^{-3}. Moreover, less than 1% of these will produce a forward going neutron or K^0_L that can simulate a photon interacting in an experimental target (assumed 2" x 2" target) so that the overall hadronic background will be less than 1.3×10^{-5} as compared to 5×10^{-3} in the present Broad Band Beam. The hadronic contamination will have roughly equal numbers of K^0_L and neutrons. Finally, it is possible to achieve further rejection of hadrons by vetoing events containing additional charged secondaries produced when the hadrons interact in the radiator.

Muon Background

The muon background in the new Broad Band experimental hall has two main component sources which are decay of π's that are generated in the primary production target and prompt muon production by hadrons. Th dominant sources of prompt muon generation are the production target, the proton dump, and the neutral dump.

The decay of π's that were generated by 1000 GeV protons in the Be target produces muons with an extremely wide momentum spectrum. Part of this momentum spectrum is within the Wide Band Beam acceptance and thus will be called beam-like muons. Many of these beam-like μ's are within the magnetic fields of the gap and the return legs of beam line devices and can be transported into the experimental hall. The

distribution of muons from this source can be calculated via the program HALO.[17] In the charged pion mode, where the beam-like muon background is most serious, the ratio of μ/π at 700 GeV is of order 10^{-4}.

Muons outside the beam phase space may nevertheless reach the experimental hall and pass through the detectors causing large singles rates and triggering problems. The fluxes of muons incident on a detector in the new experimental hall have been estimated, using a very simplified model of the beam line. A series of Monte Carlo programs, TURTLE[18] and DECAY TURTLE,[19] were applied to decay muons produced in the production target, primary beam dump, and neutral beam dump, as well as for prompt muons produced in the beam dumps. The target box geometry was modeled fairly exactly. The beam line was approximated as target box, drift space, steel shield, drift space (dipole enclosure), steel shield, and final drift space to detector plane. The 360 feet of steel shielding would produce a minimum energy cut-off of 125 GeV on produced muons. Multiple scattering and dE/dx were taken into account in tracking the muons through the steel shield.

For the neutral beam mode, the number of muons per 10^{12} primary protons incident in 1-meter-high horizontal (bend plane) strips is shown in Fig. 20a. There are three major components to this spectrum. The peaks near ± 5 meters marked μ^+ and μ^- are the tails of decay muons swept away by the target box B2 magnets. The shaded central region consists of muons produced in the aluminum dump due to decays in the aluminum and prompt muon production. There is also a small contribution from neutrons striking the neutral dump.

If we integrate the muon flux over a ± 2 meter x ± 2 meter detector aperture, we find a total of 3.7×10^6 muons/10^{12} protons with a maximum rate of 8×10^5 muons/10^{12} protons/square meter. Notice that 3.2×10^6

muons originate in the aluminum dump. The addition of 20 feet of 20 Kga magnetic dipole field just downstream of the dump will spread these muons, Fig. 20c, and lower their number by a factor of 0.71, giving a total number of muons of 2.8×10^6 $\mu/10^{12}$p and maximum rate of about $10^5\mu/10^{12}p/m^2$. The 1 TeV projected muon rate in the present Broad Band Beam is a factor of about 20 higher.

When used in the charged-beam mode, the target box B2 dipoles are run at lower current, thereby producing a narrower "hole" for the primary target decay muons. Fig. 20d shows the muon distribution when tuned for a 500 GeV π^- beam. The central maximum muon rate remaining the same at about 8×10^5 $\mu/10^{12}$ p/m^2. The wing corresponding to μ^+ at the edge of the detection plane corresponds to approximately 1.5×10^6 $\mu/10^{12}$ p/m^2, leading to a much-reduced fiducial volume and higher rates. These muons are typically around 80 GeV momentum, so slightly extra shielding will not help much. The only solution is a magnetized iron dipole around the beam line. Such an iron dipole has been built for the High Intensity Beam in P-West. Notice that toroidal spoilers will only sweep away one lobe, while focusing the other into the detector region.

VI. Photon Radiator and Electron Dump

The purpose of the photon radiator area is to produce a clean bremsstrahlung photon, to define the photon direction, and to deflect the high energy electrons which do not interact in the radiator. A 100 kG-meter "C" magnet would be required to place the non-interacting electrons onto the well-shielded electron dump. A schematic of the photon radiator area is shown in Fig. 21. In order to prevent interactions in air or windows of either the recoil electron or the bremsstrahlung photon, the beam vacuum would be continued through the "C" magnet to the experimental area. The vacuum chamber would be extended in the bend plane of the "C" magnet to avoid having a wall near the photon beam.

It is possible to have interactions in the radiator resulting in either no bremsstrahlung photon from subsequent pair production of the photon in the radiator, or a wrong direction photon resulting from Compton-electron scattering of the photon. In order to avoid triggering on decay products of such interactions, a series of anti-counters would be installed to catch the produced charged particles not going into the electron dumping cave.

A. Radiator

The radiator would be located directly upstream of the "C" magnet. It would be composed of two crossed hodoscope arrays followed by a lead foil. The purpose of the hodoscopes would be to localize the incident electron to within 1 mm both vertically and horizontally. By determining the interaction vertex at the experimental target located 30 meters downstream, the incident photon direction would be known to 0.3 mrad.

Knowledge of the photon direction is important for identifying diffractively produced coherent final states. For other physics processes the hodoscopes would not have to be used. A lead radiator would be used because of its large radiation length to interaction length ratio. This helps minimize the possibility of beam pions interacting and producing a forward neutron or a K^0_L which could in turn interact in the experimental target. It is possible to use scintillators in such high intensity beams because of the tevatron's long spill time of 20 sec. With an electron beam intensity of 10^8 e^- per 10^{12} 1 TeV protons the instantaneous rate would be only 5×10^6 electrons/sec. By spreading this flux over several counters the rate in any single counter is quite manageable.

B. Anticounters

The anticounters would be used to veto events in which there might be no bremsstrahlung photon or in which there might be a subsequent interaction of the bremsstrahlung photon. The anticounters would also be used to veto beam halo particles.

Anticounter A1 would be used to help veto hadronic interactions in the radiator and would serve to eliminate beam halo spray. Anticounters A2, A4, A5, and A6, all on the opposite side of the beam from the recoil electrons,would serve to veto positrons from trident ($e^+e^-e^-$) production in the radiator. The remaining anticounter A3 would be installed on the low energy side of the "C" magnet. In most cases A3 should be redundant with counters on the positron side of the magnet. Anticounter A3 should veto the small category of photons which Compton electron scatter and give the photon the wrong beam

direction at the experimental target.

C. Dump

The electron dump would be located 3 inches away from the photon beam and 20 meters downstream of the radiator. It would consist of a central core of hevimet (tungsten alloy), followed by 12 feet of steel. The steel would be used to range out 5 GeV muons from $\mu^+\mu^-$ pair production in the dump. This would reduce μ rate per incident 700 GeV e^- below 10^{-5}.

VII. Experimental Hall and Facilities

Fig. 3 shows a plan view of a possible experimental hall and service building. The service building also provides space for experimental counting rooms. An important feature of the proposed hall is that it is designed to support exactly two experiments. Previous experience in Proton-East, West and in other beam lines at Fermilab indicates that two experiments can efficiently use a single beam line which runs $\gtrsim$ 30 weeks per year. More than two experiments frustrates the ambitions of each experiment and represents an over-commitment of equipment and manpower relative to the possible available beam time.[20]

VIII. Construction Schedule

We assume that construction funds become available in October 198N. The following schedule indicates that an experiment could begin in Summer of 198(N+3) or ∿ 2½ years later:

a) Experimental Hall Complete and Ready for Occupancy	Spring 198(N+2)
b) Dipole Enclosure, EE4 addition, and Lambertson Enclosure K	Summer 198(N+2)
c) Beam Line Component Installation	Fall 198(N+2)
d) Commission Beam	Winter-Spring 198(N+3)
e) Begin Experiment	Summer 198(N+3).

IX. Summary

In the last few years, a major emphasis of the experimental program in both the Tagged Photon Beam and the Broad Band Beam has been charm spectroscopy. If there are still important questions about charm spectroscopy or production, this beam with its high flux of photons will be an ideal place to conduct experiments to get the answers. Similarly, the high intensity and energy is crucial to any search for states with beautiful quarks.

On the other hand, it is always difficult to predict several years in advance what direction the fixed-target program will take. The physics workshops anticipating the start of the 400-GeV program make little or no mention of charm and beauty, the subjects that have received much of our attention in the last 5 years. However, certain tendencies seem clear:

(i) We will be interested in very rare (small cross section) processes which reveal the innermost structure of hadrons.

(ii) The final states we investigate will be even more complex and the amount of information we want about individual events will increase.

(iii) The pressure on the experimental facilities will increase as complex experiments require more beam time for debugging and data-taking, and other programs, such as the collider, begin to compete for running time.

The proposed beam is well suited to the challenging conditions of this period. It is capable of producing the high fluxes of photons or hadrons required to observe rare processes. Because of the splitting station in P-East, experiments can be debugged with beam using very modest numbers of primary protons, while the Tagged

Beam can be the primary user. Similarly, the Tagged Photon Lab will be able to receive some beam while the Wide Band Beam is running. The new beam is a very efficient transporter of charged pions or neutrons, so that sensitive experiments using incident hadrons can be performed with primary proton requirements of only a few 10^{11}/pulse. The reduction of hadronic backgrounds will greatly simplify photon experiments.

These considerations encourage us to believe that this new beam will be the source of important contributions to physics in the Tevatron Era.

ACKNOWLEDGEMENT

We would like to thank:

F. Browning, L, Kula, A. Skraboly, G. Smith,

B. Edmonson and P. Mascione for their tireless

dedication and technical assistance.

REFERENCES

1) L. Kluberg et al., Phys. Rev. Letters 37, 1451 (1976).
D. Antreasyan et al., Phys. Rev. Letters 38, 112 (1977).
D. Antreasyan et al., Phys. Rev. Letters 38, 115 (1977).
L. Kluberg et al., Phys. Rev. Letters 38, 670 (1977).
D. Antreasyan et al., Phys. Rev. Letters 39, 906 (1977).

2) C. Halliwell et al., Nuc. Inst. and Methods 102, 51 (1972).

3) G. Gladding and M. Gormley, Performance of the Wide-Band Neutral Beam, Proton Department Internal Document (unpublished).

4) R. M. Egloff et al., Phys. Rev. Lett. 43, 657 (1979).
R. M. Egloff et al., Phys. Rev. Lett. 43, 1545 (1979).
M. S. Atiya et al., Phys. Rev. Lett. 43, 1691 (1979).

5) B. Knapp et al., Phys. Rev. Lett. 34, 1040 (1975).

6) D. O. Caldwell et al., Phys. Rev. Lett. 40, 1222 (1978).
D. O. Caldwell et al., Phys. Rev. Lett. 42, 553 (1979).

7) M. Binkley et al., Phys. Rev. Lett. 37, 571 (1976).
M. S. Atiya et al., Phys. Rev. Lett. 43, 414 (1979).
P. Avery et al., submitted to Phys. Rev. Letters Feb. (1980).

8) M. Binkley et al., Phys. Rev. Lett. 37, 571 (1976).

9) M. Binkley et al., Phys. Rev. Lett. 37, 578 (1976).

10) G. Brianti and N. Doble CERN/SPSC/77-72.
P. Astbury et al., CERN/SPSC/77-116, I98.
P. Astbury et al., CERN/SPSC/78-76, P109.

11) F. Browning et al., Proton Area Enclosure H Upgrade Projects, Fermilab TM-957 (1980).

12) B. Cox et al., P-West High Intensity Area, Secondary Beam Area Design Report Fermilab (1977).

13) M. Bourquin et al., Nuclear Physics B114, 334 (1976).

14) M. R. Whalley et al., Inclusive Neutron Production, Paper submitted to the 16th International Cosmic Ray Conference, Kyoto, Japan, August 6-18, 1979.

15) R. T. Edwards et al., Phys. Rev. D18, 76 (1978).

16) G. Giacomelli, Rapporteur talk at Chicago Conference (1972), Vol. 3, p. 219.

17) Ch. Iselin, CERN 74-17 (1974).

18) D. C. Carey, NAL-64, (1978).

19) K. L. Brown et al., CERN 74-2 (1974).

20) B. Cox, H. Frisch, M. Schochet, R. Webb, and M. Witherell, private communications.

TABLE I

SECONDARY BEAM TRANSPORT ELEMENTS

Position[a] (Ft.)	Name	Size & Type[b] (In.)	Field Strength at Pole Tip[c] (kG)	Function
0	Be target (Tp)	18 in long		Produces γ's or hadrons
0	B2-1	4-2-240	-	Sweep charged particles into the target box dump. See Fig. 9
	B2-2	4-2-240	-	
50	Q1A1	4Q120	- 8.77	First stage quad triplet produces a dispersed image at the momentum slit
61	Q1A2	4Q120	- 8.77	
94	Q1B1	4Q110	10.21	
105	Q1B2	4Q120	10.21	
116	Q1B3	4Q120	10.21	
149	Q1C1	4Q120	- 8.77	
160	Q1C2	4Q120	- 8.77	
171	B1A	6-3-120	16.36	Produce dispersion and bend beam away from 0^0 line.
182	B1B	6-3-120	16.36	
452	Collimator	5-3	-	Momentum slit for momentum definition.
462	B2A	6-3-120	-16.36	Cancel dispersion.
473	B2B	6-3-120	-16.36	
484	B2C	6-3-120	-16.36	
495	B2D	6-3-120	-16.36	
775	B3A	6-3-120	16.36	Recombine momentum dispersi and make beam achromatic.
786	B3B	6-3-120	16.36	
797	Q2A1	4Q120	8.54	Second state quad triplet produces achromatic image at experimental target.
808	Q2A2	4Q120	8.54	
833	Q2B1	4Q120	-10.16	
844	Q2B2	4Q120	-10.16	
855	Q2B3	4Q120	-10.16	
880	Q2C1	4Q120	8.54	
891	Q2C2	4Q120	8.54	
903	Pb Radiator			Produces bremsstrahlung photon beam.
906	Radiator "C"	180 in long	-22	Sweep and dump electrons.
1001	Target (Texp)			Experimenters target.

a = Position at upstream face of element.
b = Horizontal - vertical dimensions transverse to beam.
c = For quads negative field means vertical focusing.

TABLE II

SECONDARY BEAM PROPERTIES

ACCEPTANCE PARAMETERS

$\delta x = \pm 1$ mm	- Horizontal spot size of source
$\delta y = \pm 1$ mm	- Vertical spot size of source
$\delta\theta_x = \pm 1.0$ mrad	- Geometric horizontal angle accepted
$\delta\theta_y = \pm 0.75$-$\pm 1.0$ mrad*	- Geometric vertical angle accepted
$\delta\Omega = 3$-4μster*	- Geometric solid angle accepted
$\frac{\Delta P}{P} = \pm 15\%$	- Momentum bite accepted
$\delta\Omega\frac{\delta P}{P} = 120\mu$ster%	- Beam acceptance via Monte Carlo program

BEAM PARAMETERS AT TARGET

$\delta x = \pm 1.25$ cm	- Horizontal beam spot at experimental target
$\delta y = \pm 0.75$ cm	- Vertical beam spot at experimental tarç
$\delta\theta_x = \pm 0.5$ mrad	- Horizontal divergence at experimental target
$\delta\theta_y = \pm 0.6$ mrad	- Vertical divergence at experimental target

*Depends on choice of target box collimator

TABLE III

P-EAST 2-WAY SPLIT

Element	Location (Enclosure)	Function
1) Eartly Trim	H	Adjust beam split ratio. Field is 15 Kg-m. Distance to first septum is 115'. Maximum motion of beam is 5/8".
2) Quadrupole Doublet (2 EPB Dipoles)	H	Focus beam onto aperture of Lambertson magnets in Enclosure K. Spot is ± 1/4".
3) Eartly Trim	H	Adjust angle of attack of beam on septum wires to minimize losses.
4) 4 Electrostatic Septa (3.1 m, 2 cm gap, 70 KV, Double Cathode)	H	Separate the protons falling on opposite sides of the wires into two divergent beams. Total deflection of each beam is 0.044 mrad. Beam separation at aperture of first Lambertson magnet in Enclosure K is 1.1".
5) Eartly Trim	H	Adjust position of two beams at entrance to Lambertson's in Enclosure K.
6) Trim	K	Magnetic compensation for vertical deflection of beam due to electrostatic septa. Used to bring the beam in along the correct line at the pretarget area.
7) 3 Two-Way Lambertson Magnets	K	Pass beam to Tagged Photon Line without deflection. Bend beam to Wide Band Line through 2.1 mrad to east.

TABLE IV

PRE-TARGET ELEMENTS

Element*	Location (Distance from center line to production target in feet)	Function
1) 4 ED/s Dipoles	256' (EE1)	Bends primary beam east by 300 mr to separate it from Tagged Photon beam.
2) 6 ED/s Quadrupoles	145' (EE1)	Quadrupole doublet to form parallel-to-point focus in both planes on production target in EE4.
3) EPB Dipole	111.5' (EE1)	Pitching magnet for dog-leg to adjust beam position and angle on production target. Bend is in vertical plane. Maximum angle = 1.5 mrad
4) 2 Main Ring Dipoles (B2)	25' (EE4)	Pitching magnets for dog-leg to adjust beam position and angle in production target. Bend is in vertical plane. Maximum angle = 6.4 mrad
5) 1.2 Collision Length Be production target	0' (EE4)	

* Numbers correspond to those on elements of fig. 8

TABLE V

NEUTRON YIELDS

Incident Proton Energy	Angular Acceptance (mrad x mrad)	Spot Size (in x in)	Yield Neutrons Incident Proton
400 (present beam)	0.625 x 0.0313	.33 x .17	7.1×10^{-6}
	0.14 x 0.07	.75 x .375	3.5×10^{-5}
	0.167 x 0.167	.90 x .90	9.9×10^{-5}
1000 (new beam)	0.0625 x 0.0313	.75 x .375	4.4×10^{-5}
	0.14 x 0.07	1.50 x .75	2.1×10^{-4}
	0.167 x 0.167	2.0 x 2.0	5.9×10^{-4}

TABLE VI

TYPICAL WIDE BAND BEAM YIELDS FOR

INCIDENT 1 TEV PROTONS

Particle	Energy	Yield/10^{12}
e^-	450 GeV 600 GeV	6×10^7 1×10^7
γ	$E\gamma > 200$ GeV	7.5×10^6
n	Spectrum as in Section IV	6×10^8
K^0_L	Spectrum as in Section IV (7 collision lengths)	1×10^5
p	1000 GeV	2×10^9
π^-	600 GeV	1.5×10^9

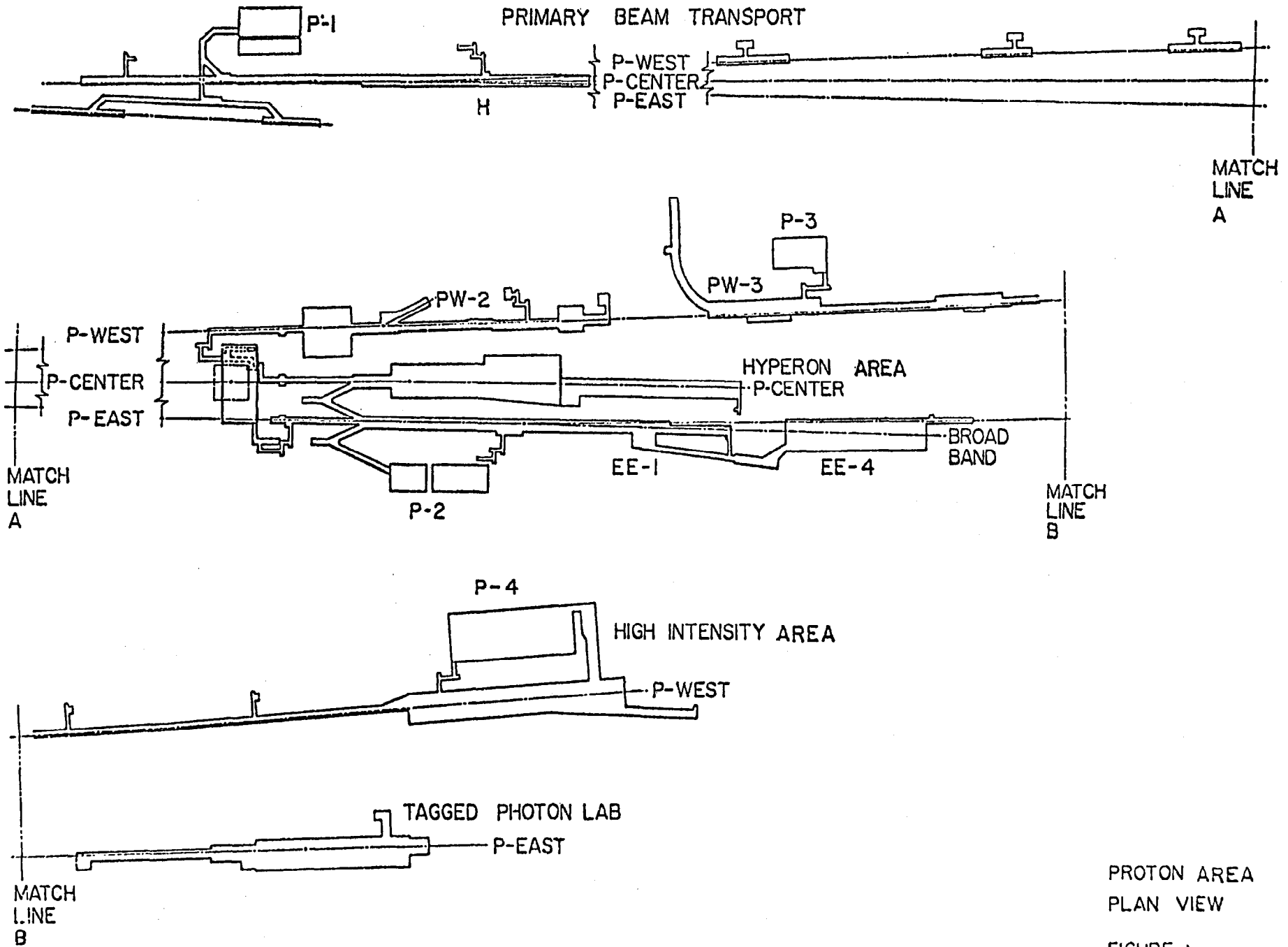

PROTON AREA
PLAN VIEW

FIGURE 1

TM-963

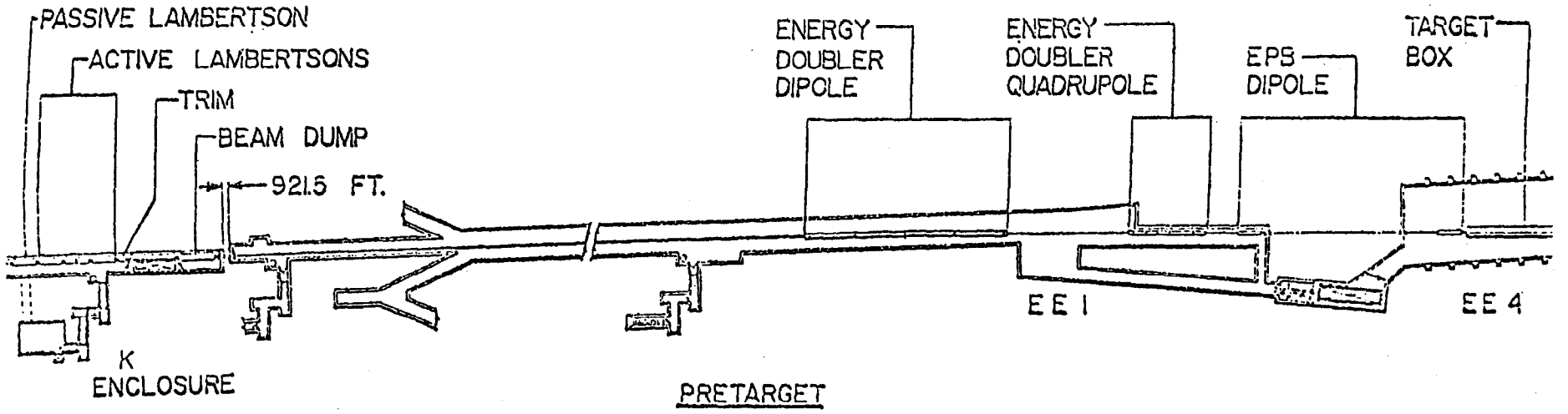

PRETARGET

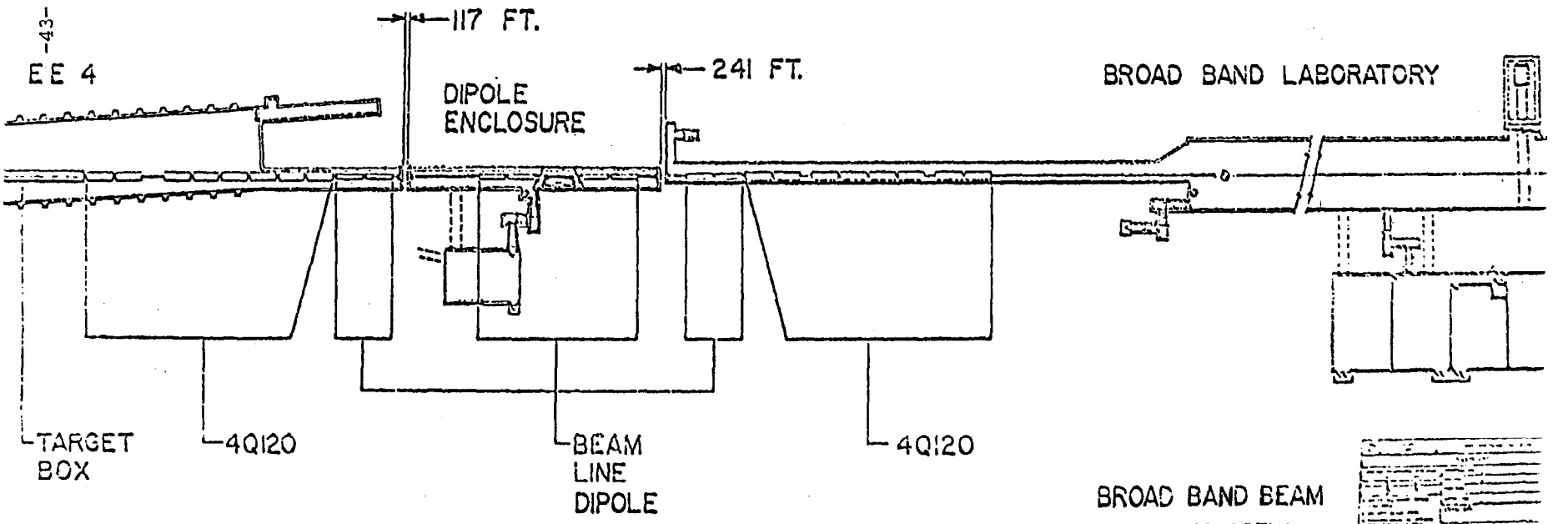

POST TARGET

BROAD BAND BEAM PLAN VIEW

FIGURE 2

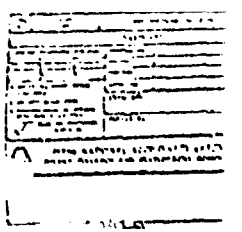

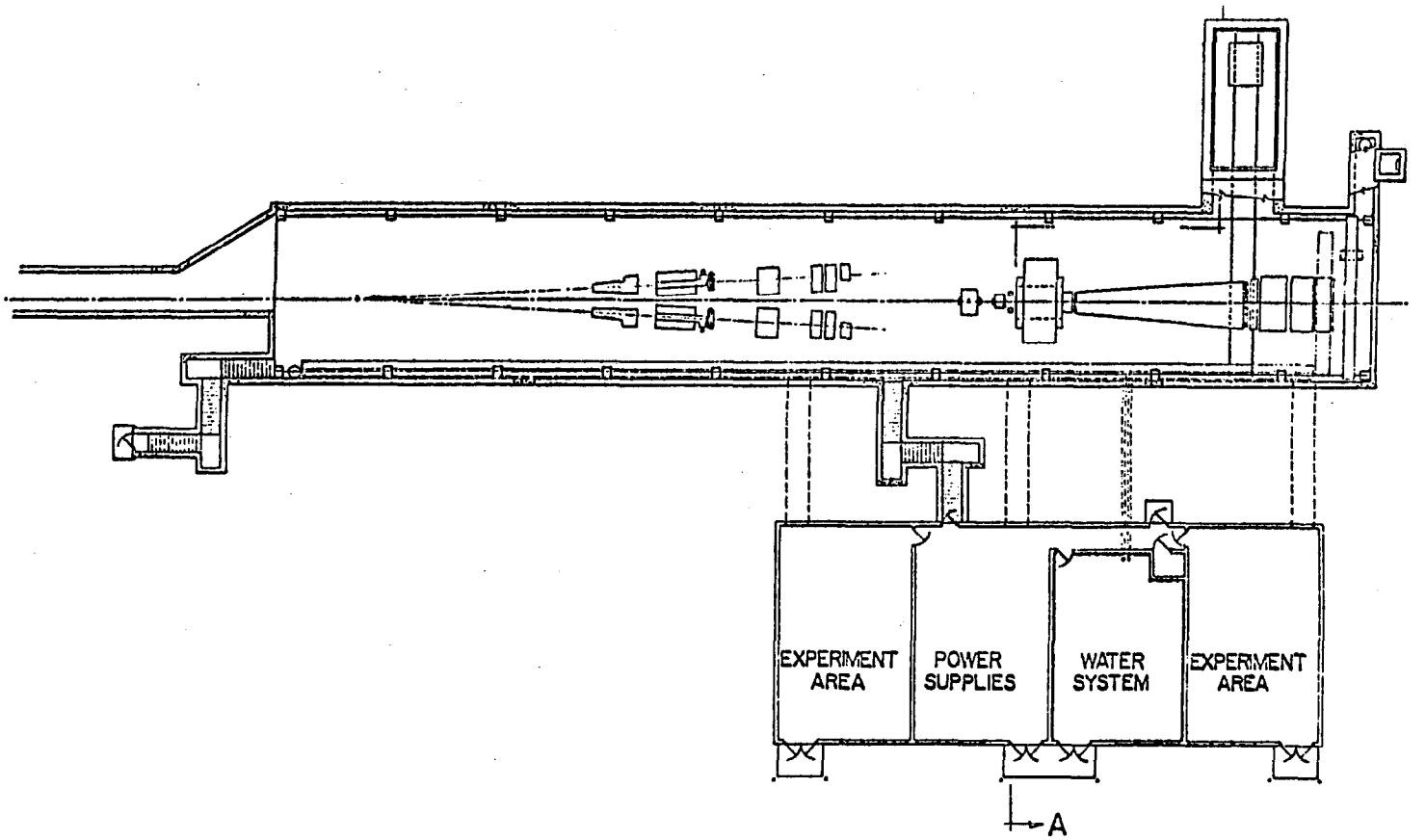

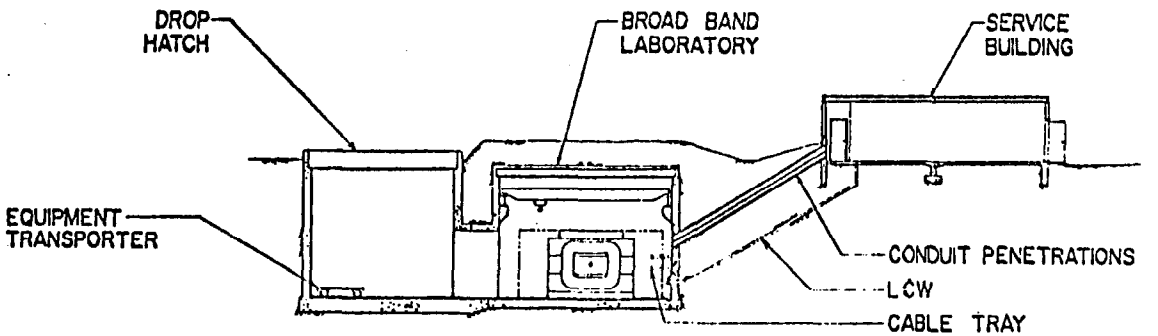

SECTION A-A

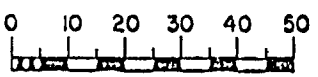

FIGURE 3

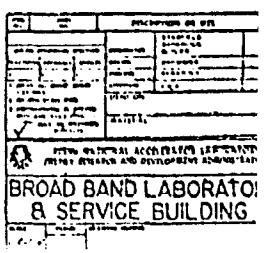

TM-963

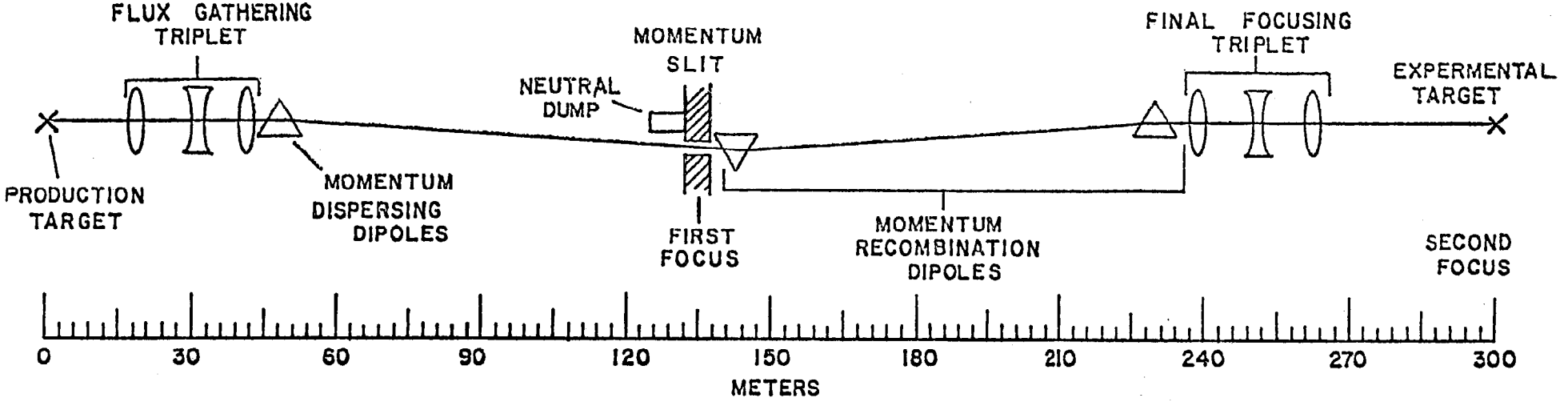

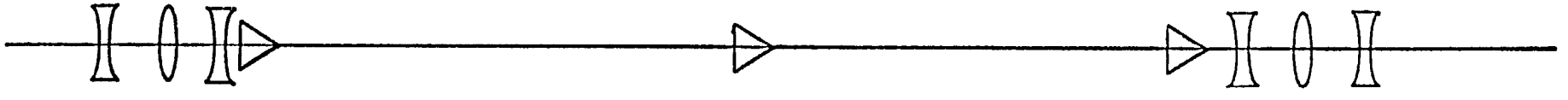

BROAD BAND BEAM
OPTICS DIAGRAM
1 TeV

FIGURE 4

TM-963

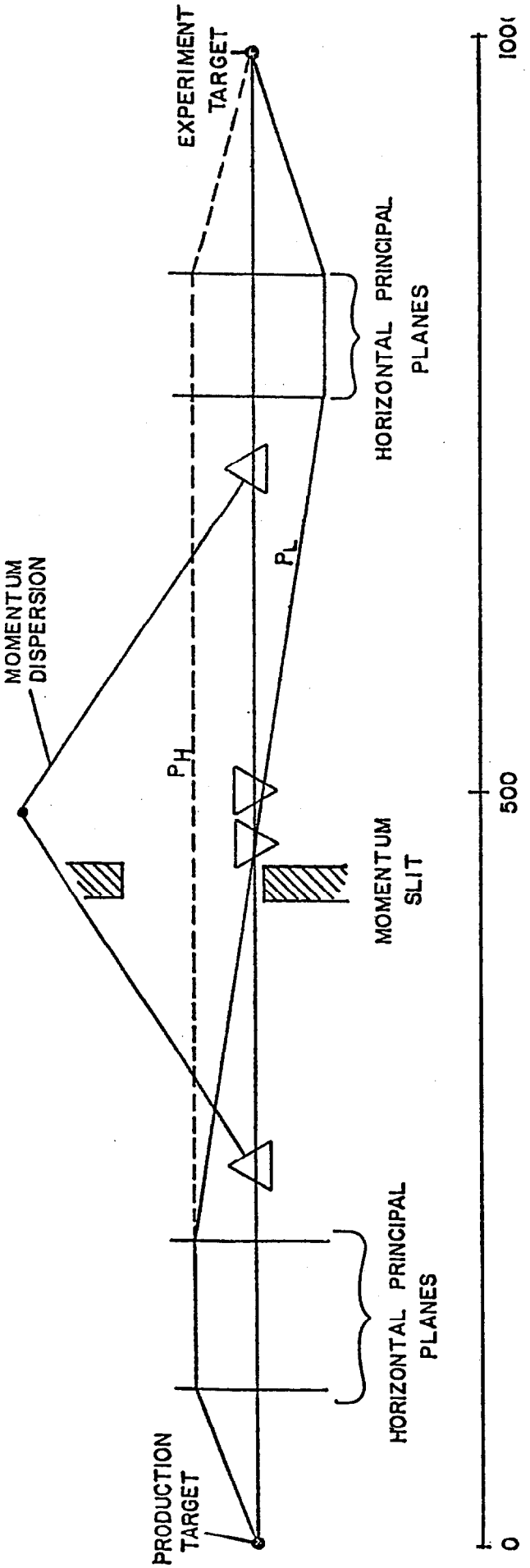
EXPERIMENT TARGET
HORIZONTAL PRINCIPAL PLANES
MOMENTUM DISPERSION
P_L
P_H
MOMENTUM SLIT
HORIZONTAL PRINCIPAL PLANES
PRODUCTION TARGET
0
500
DISTANCE FROM PRODUCTION TARGET (IN FEET)

FIGURE 5

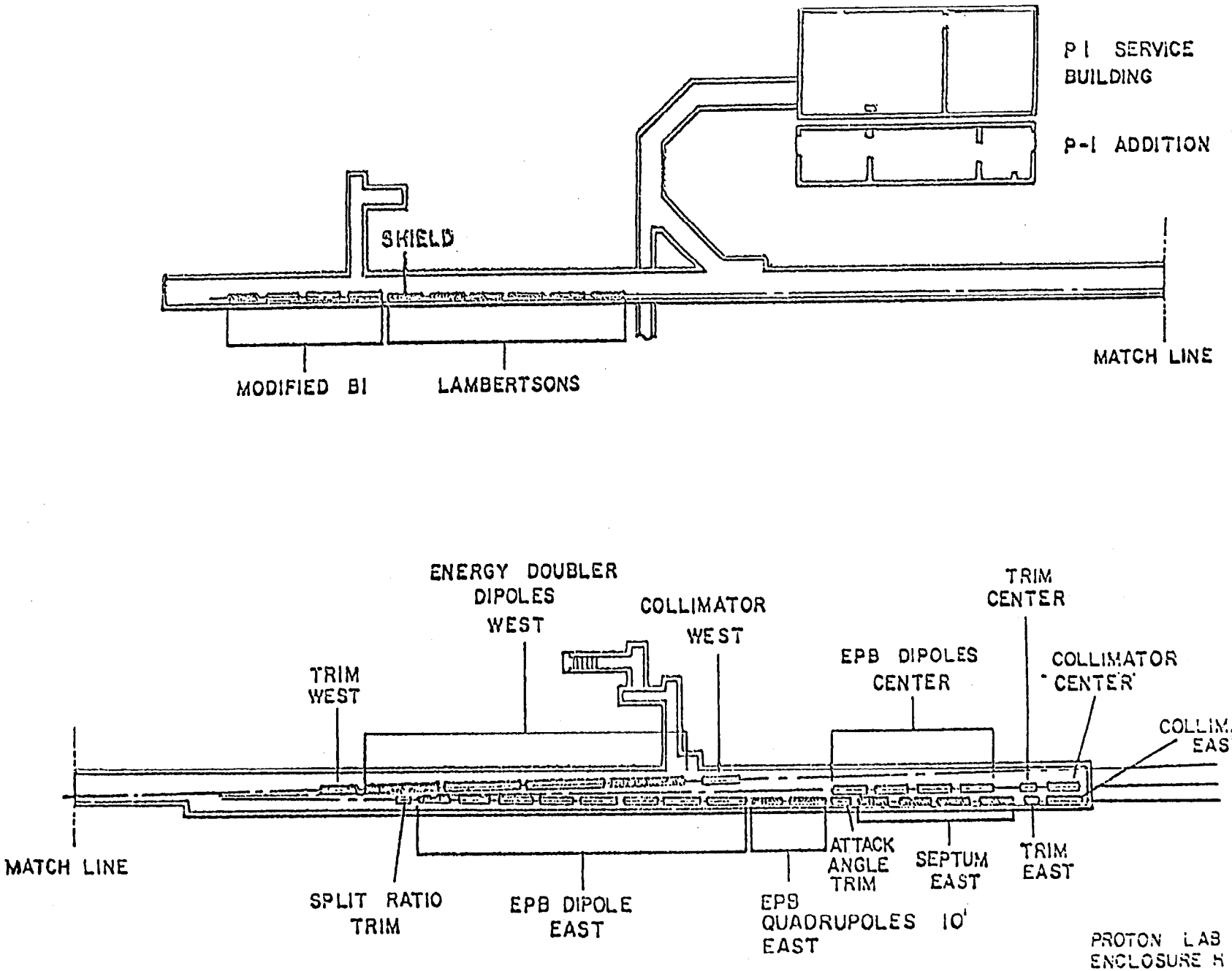

ELEMENTS NEEDED FOR TEV II PROJECT

PROTON LAB
ENCLOSURE H
I TEV CONFIGURATION

FIGURE 6

TM-963

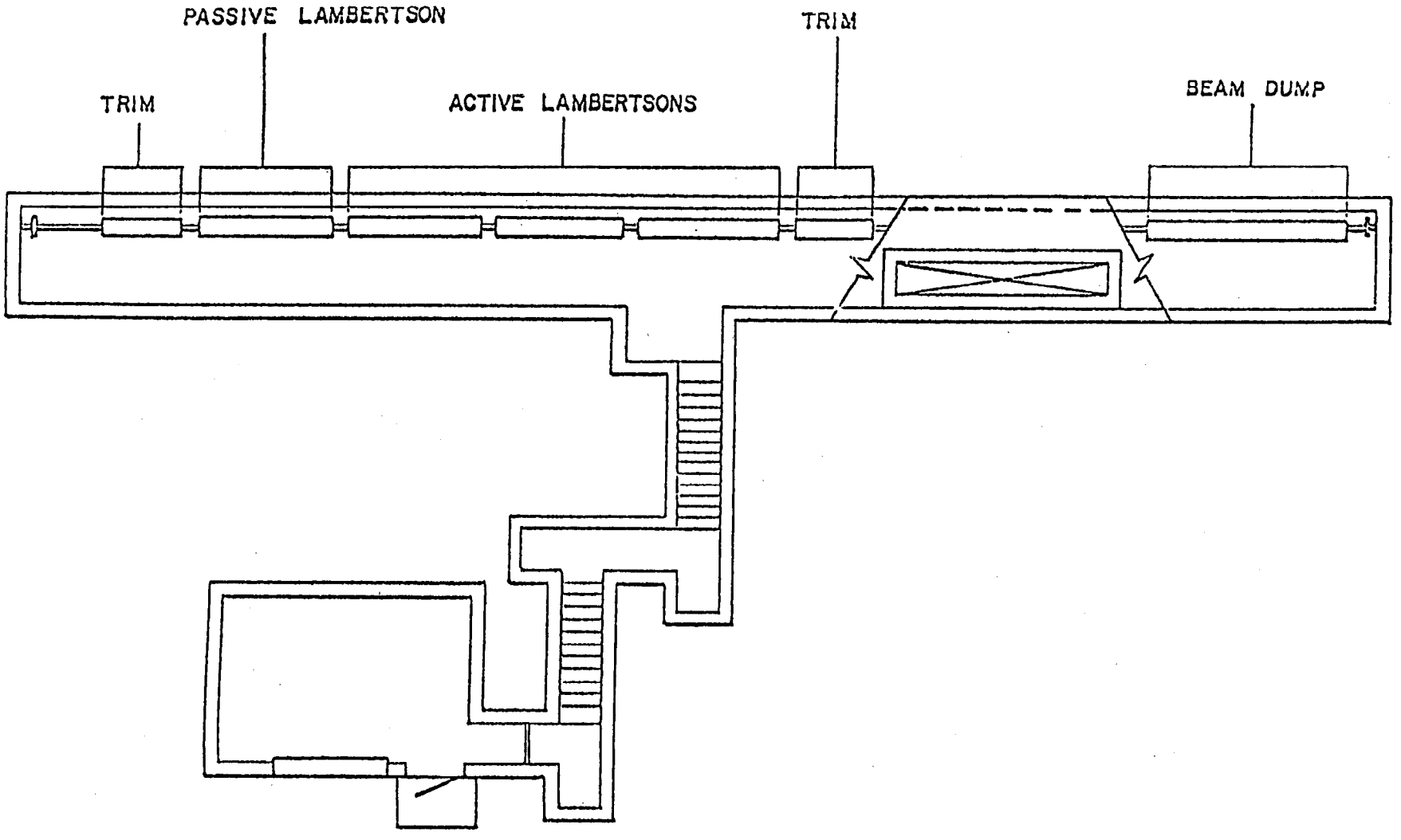

PROTON EAST
K ENCLOSURE
FIGURE 7

TM-963

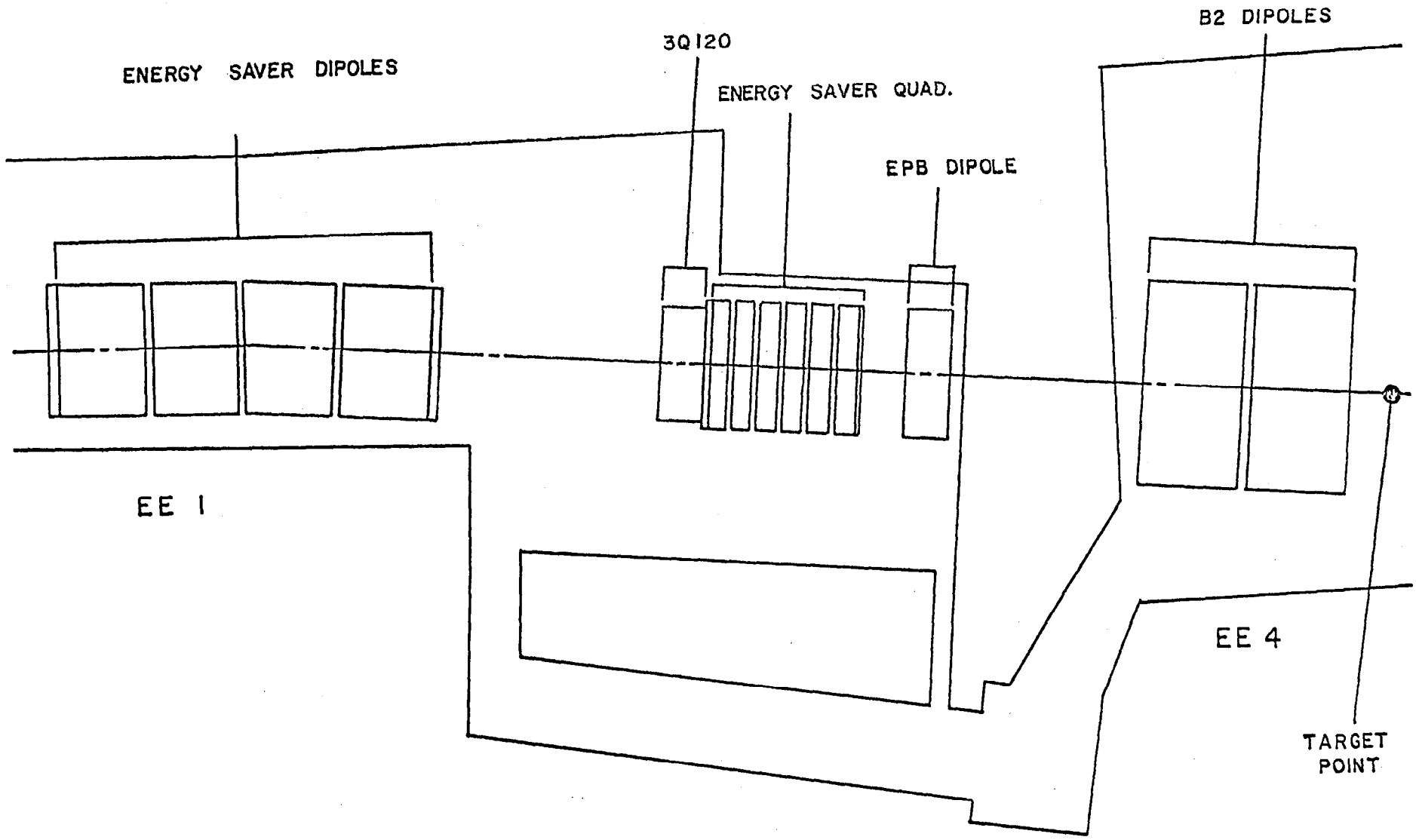

FIGURE 8 BROAD BAND PRE TARGET

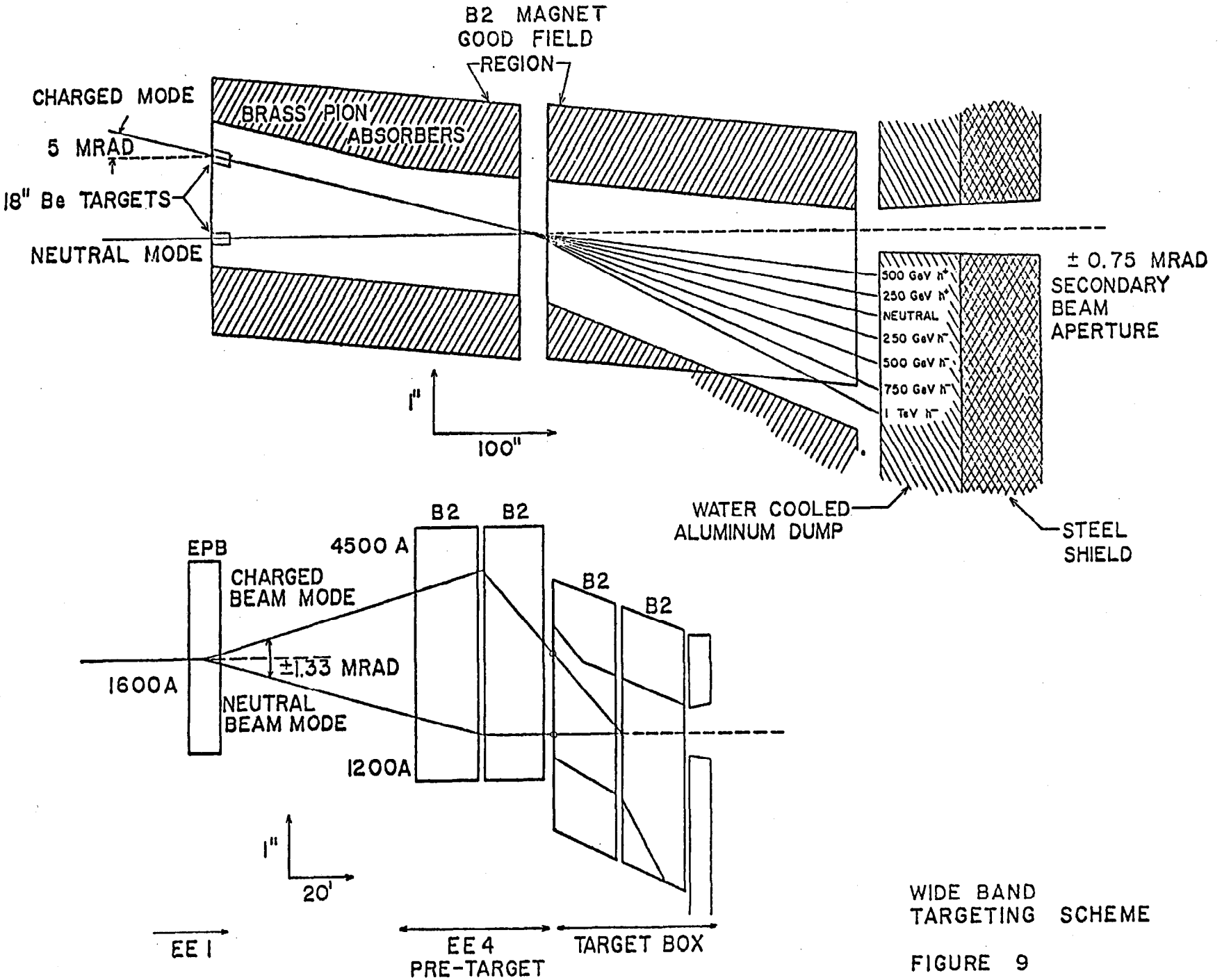

WIDE BAND
TARGETING SCHEME

FIGURE 9

TM-963

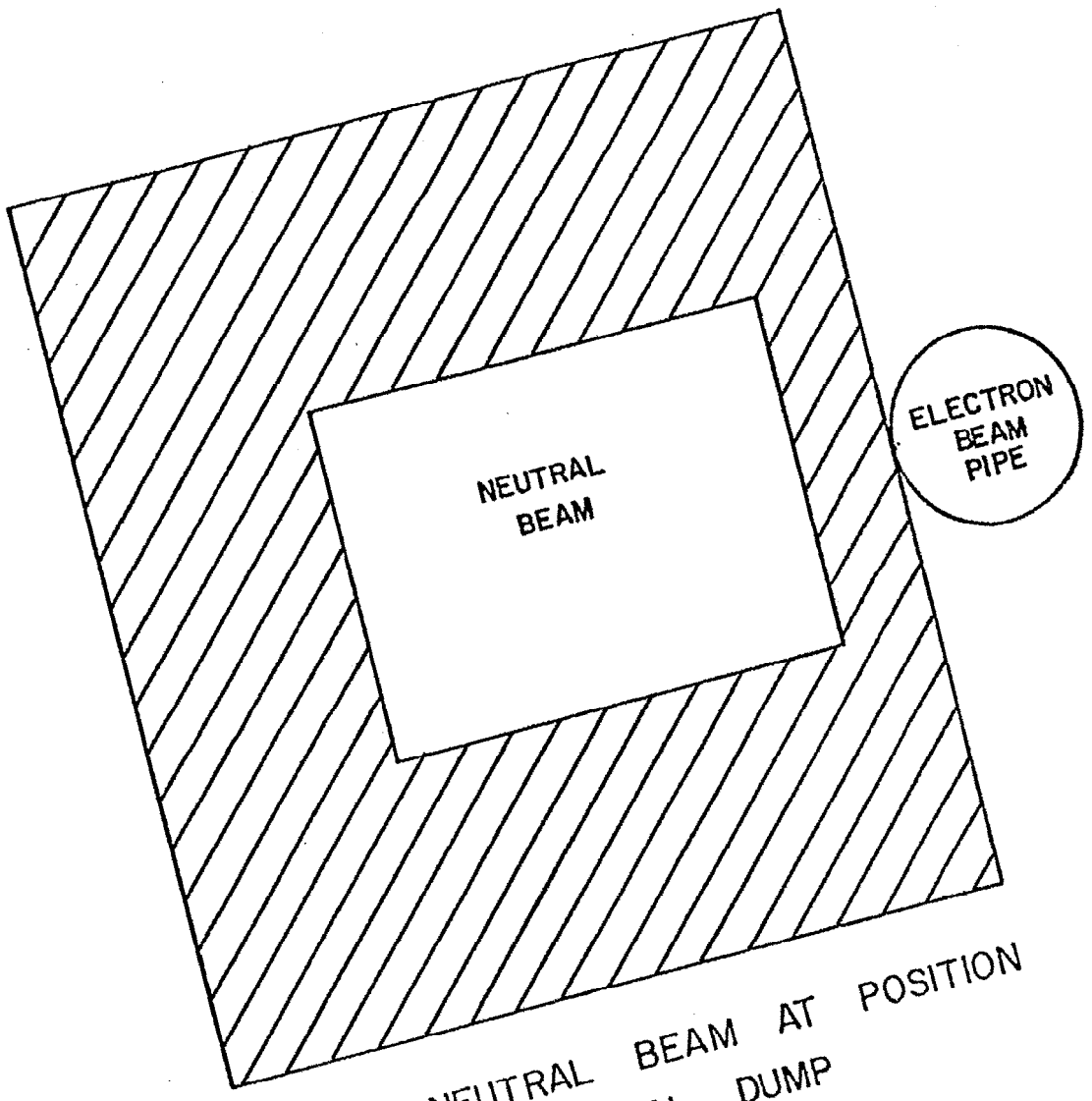

FIGURE 10a: NEUTRAL BEAM AT POSITION OF NEUTRAL DUMP

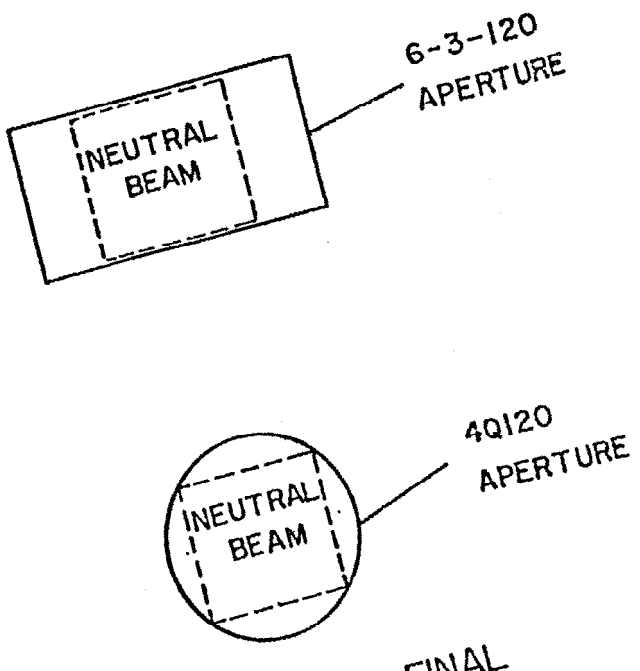

FIGURE 10b: NEUTRAL BEAM AT FINAL FIRST STAGE ELEMENTS

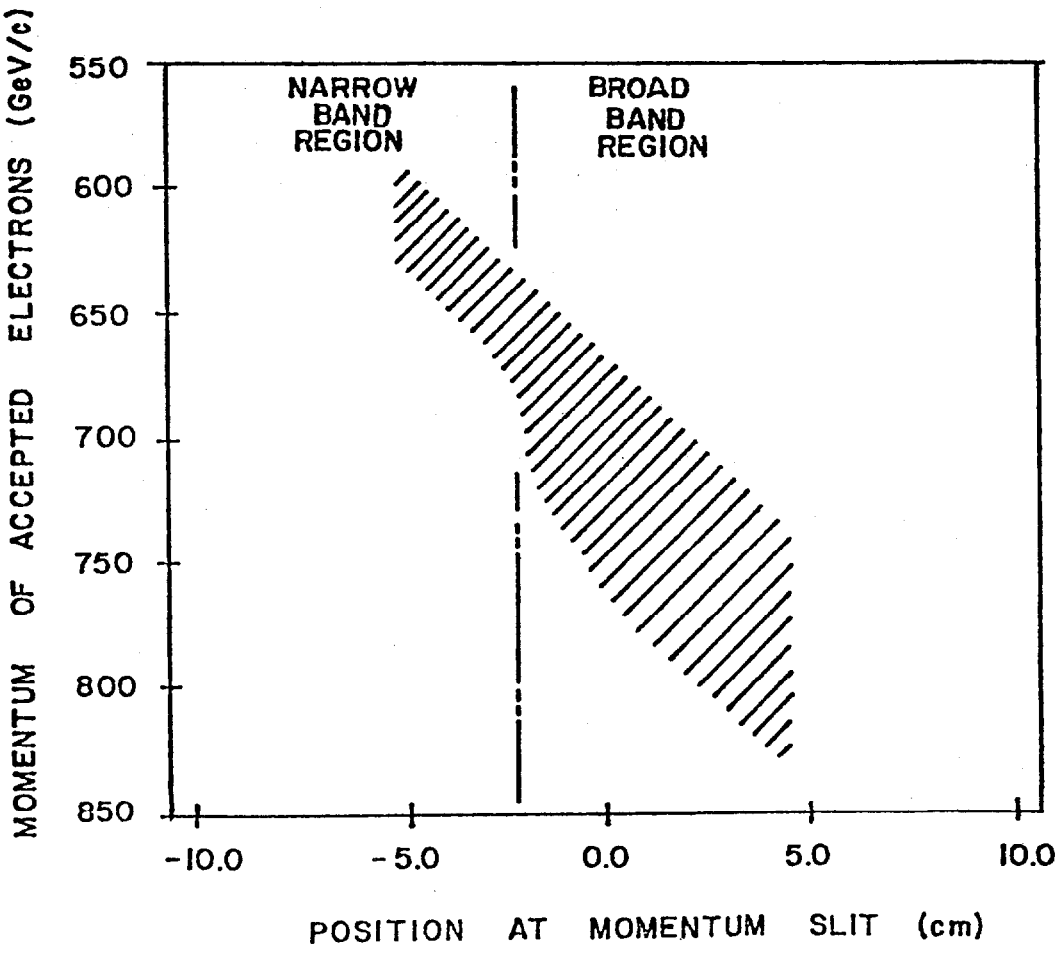

FIGURE 11: PROPERTIES OF BEAM AT MOMENTUM SLIT

RELATIVE PHOTON YIELD VS TARGET THICKNESS

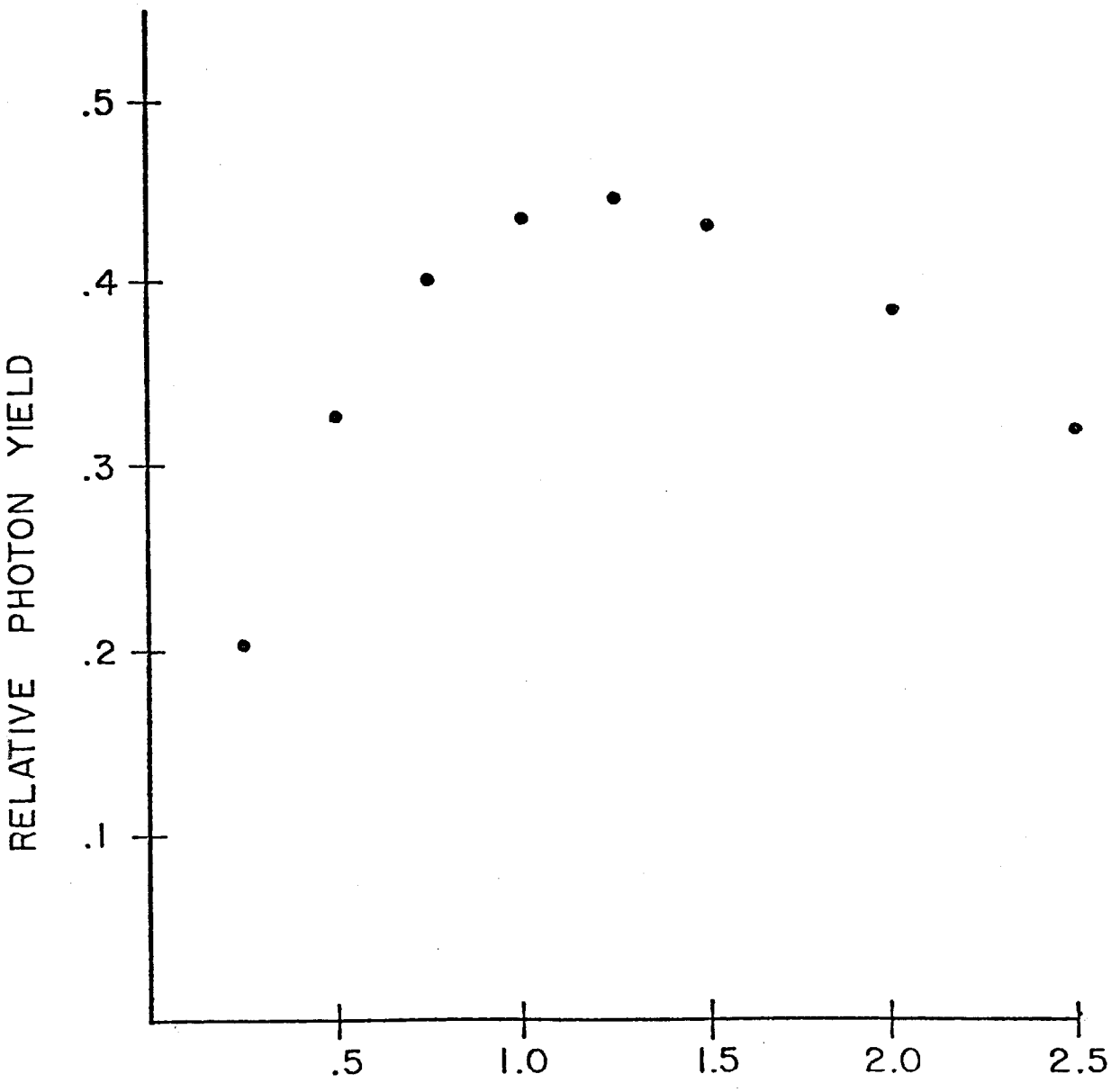

FIGURE 12A

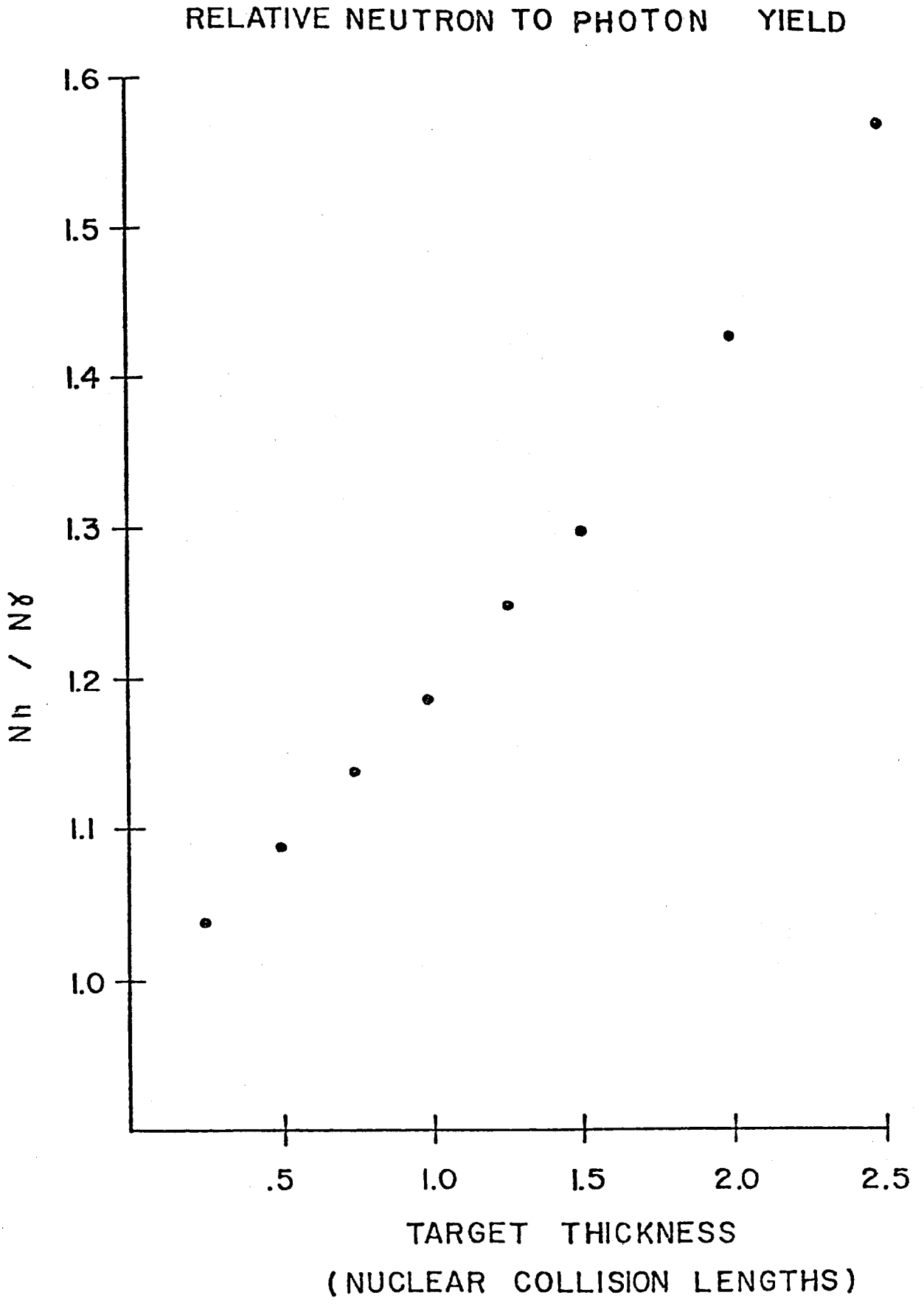
RELATIVE NEUTRON TO PHOTON YIELD
1.6
1.5
1.4
1.3
1.2
1.1
1.0
Nh / Nγ
.5
1.0
1.5
2.0
2.5
TARGET THICKNESS
(NUCLEAR COLLISION LENGTHS)

FIGURE 12B

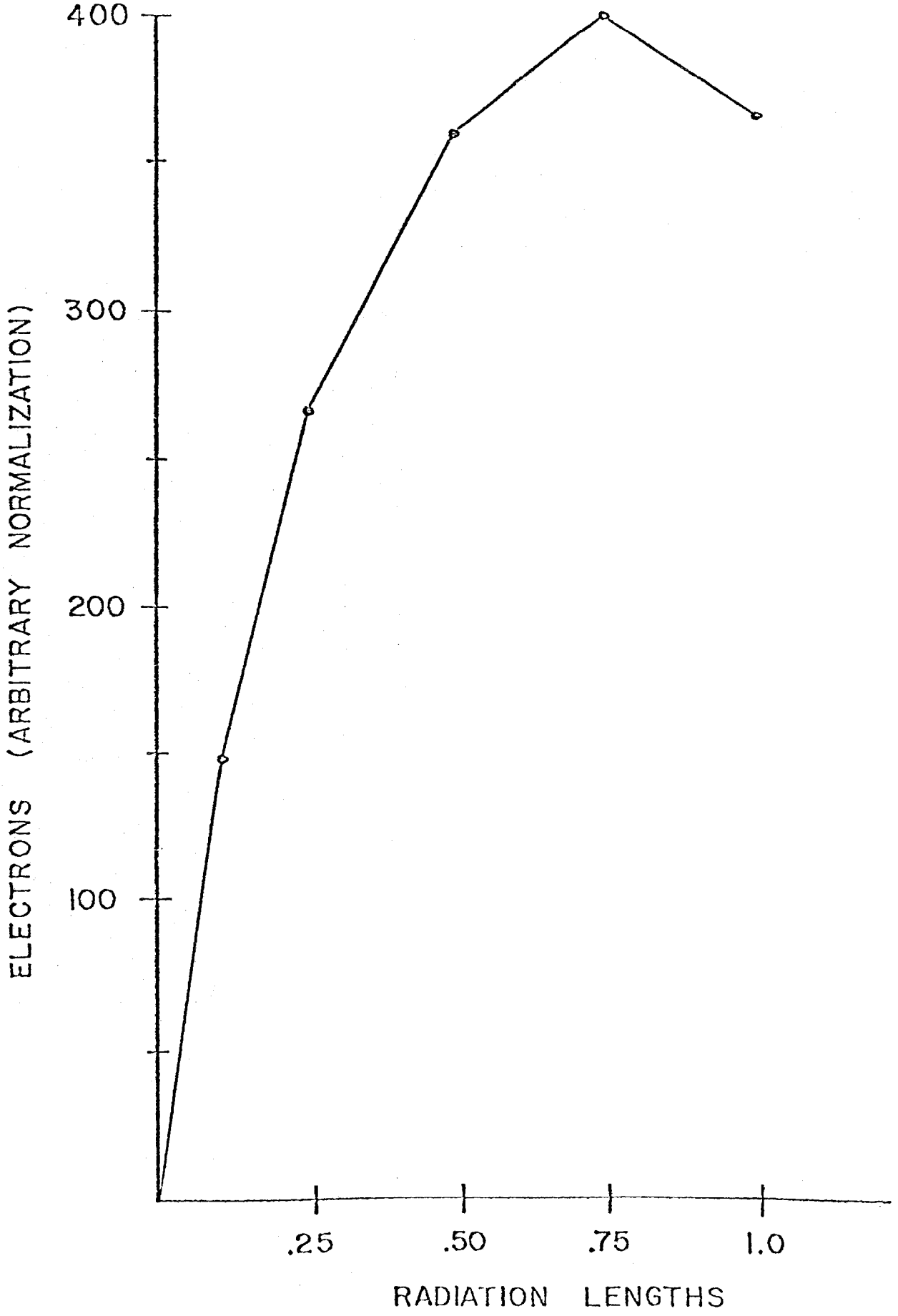
400
300
200
100
ELECTRONS (ARBITRARY NORMALIZATION)
.25
.50
.75
1.0
RADIATION LENGTHS

FIGURE 13

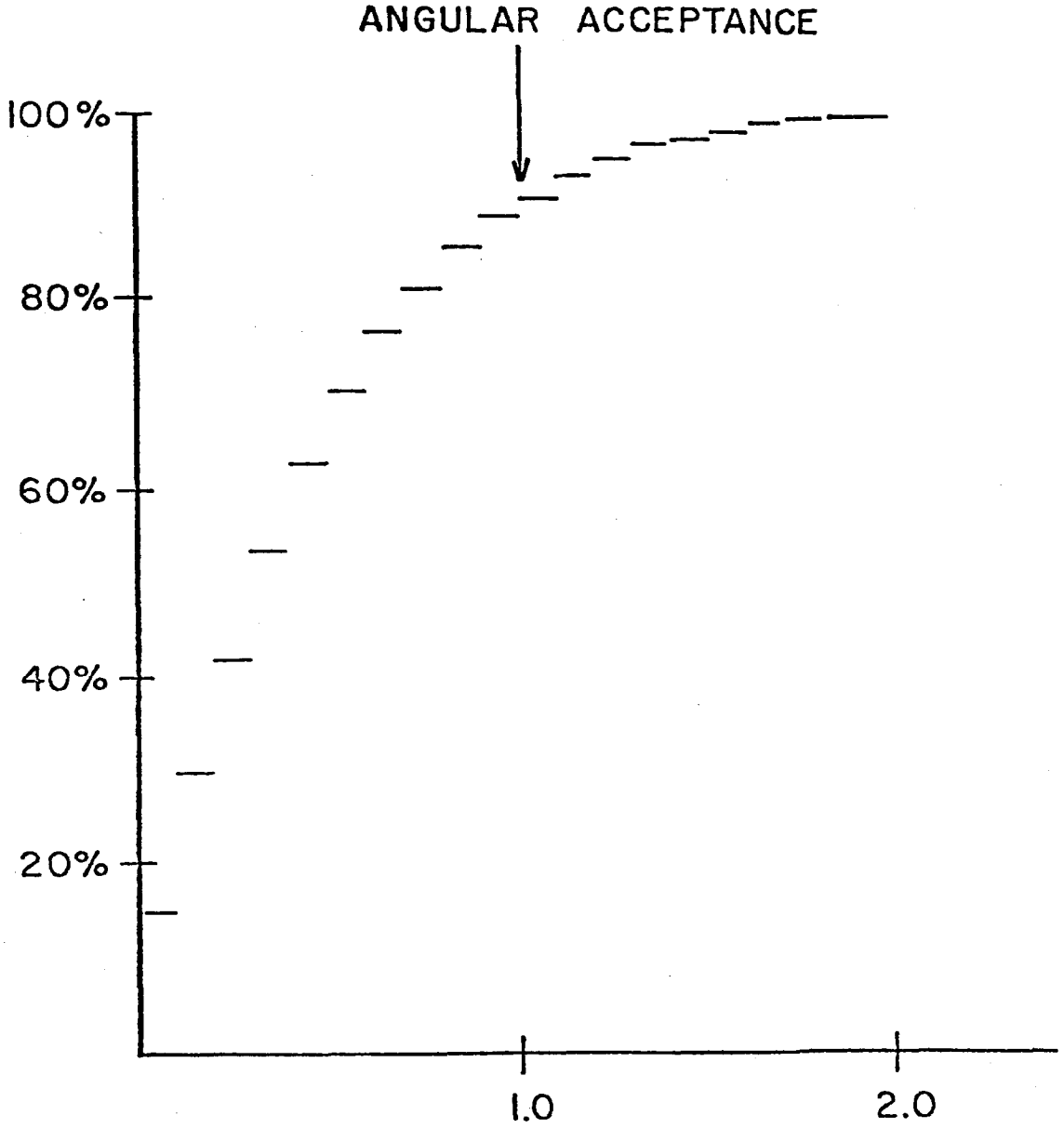

FRACTION OF PION YIELD PRODUCED
AT ANGLES LESS THAN $\theta \times \{MR\}$
AND MOMENTA >350 GeV/C

FIGURE 14

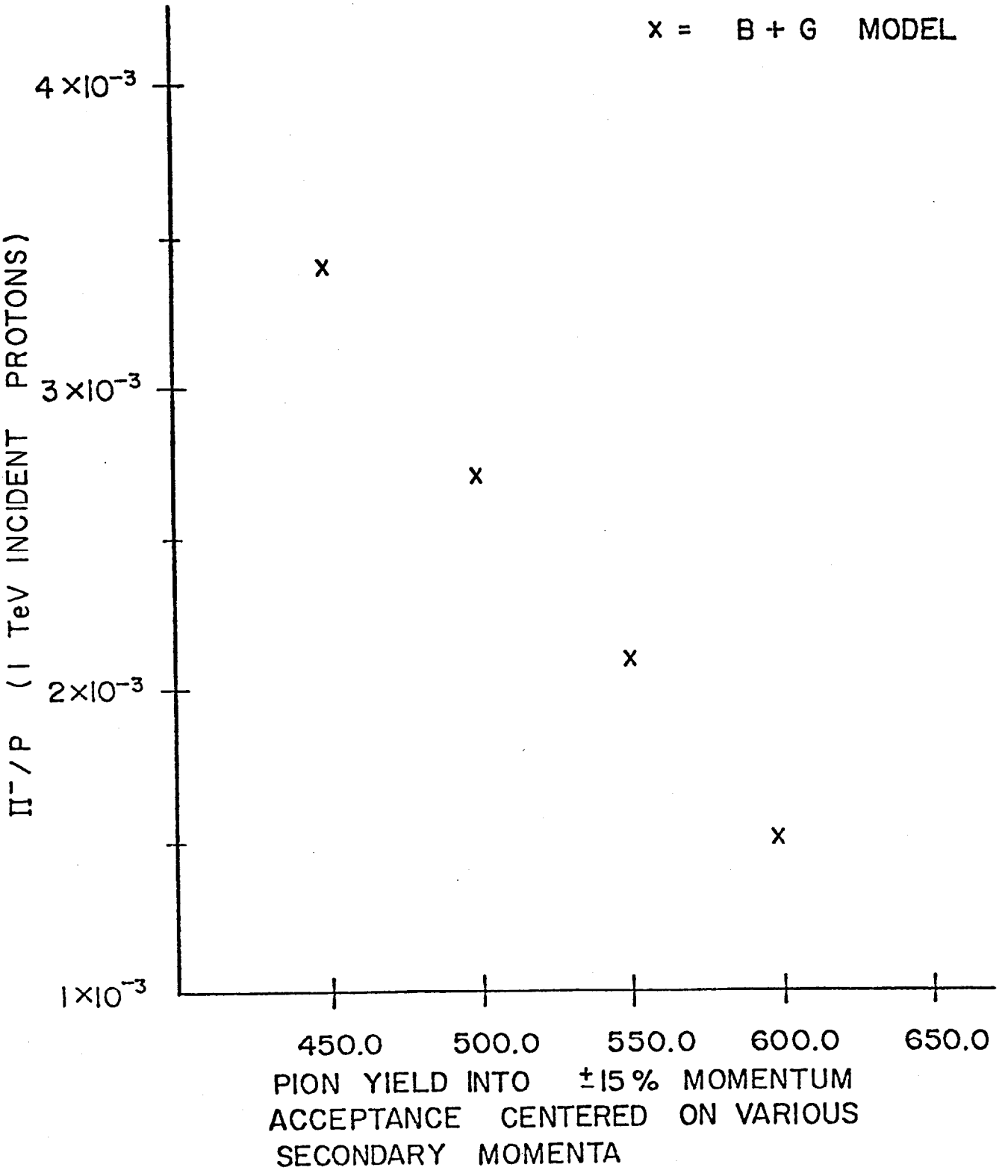
x = B + G MODEL
4×10⁻³
3×10⁻³
2×10⁻³
1×10⁻³
Π⁻/P (1 TeV INCIDENT PROTONS)
450.0
500.0
550.0
600.0
650.0
PION YIELD INTO ±15% MOMENTUM ACCEPTANCE CENTERED ON VARIOUS SECONDARY MOMENTA

FIGURE 15

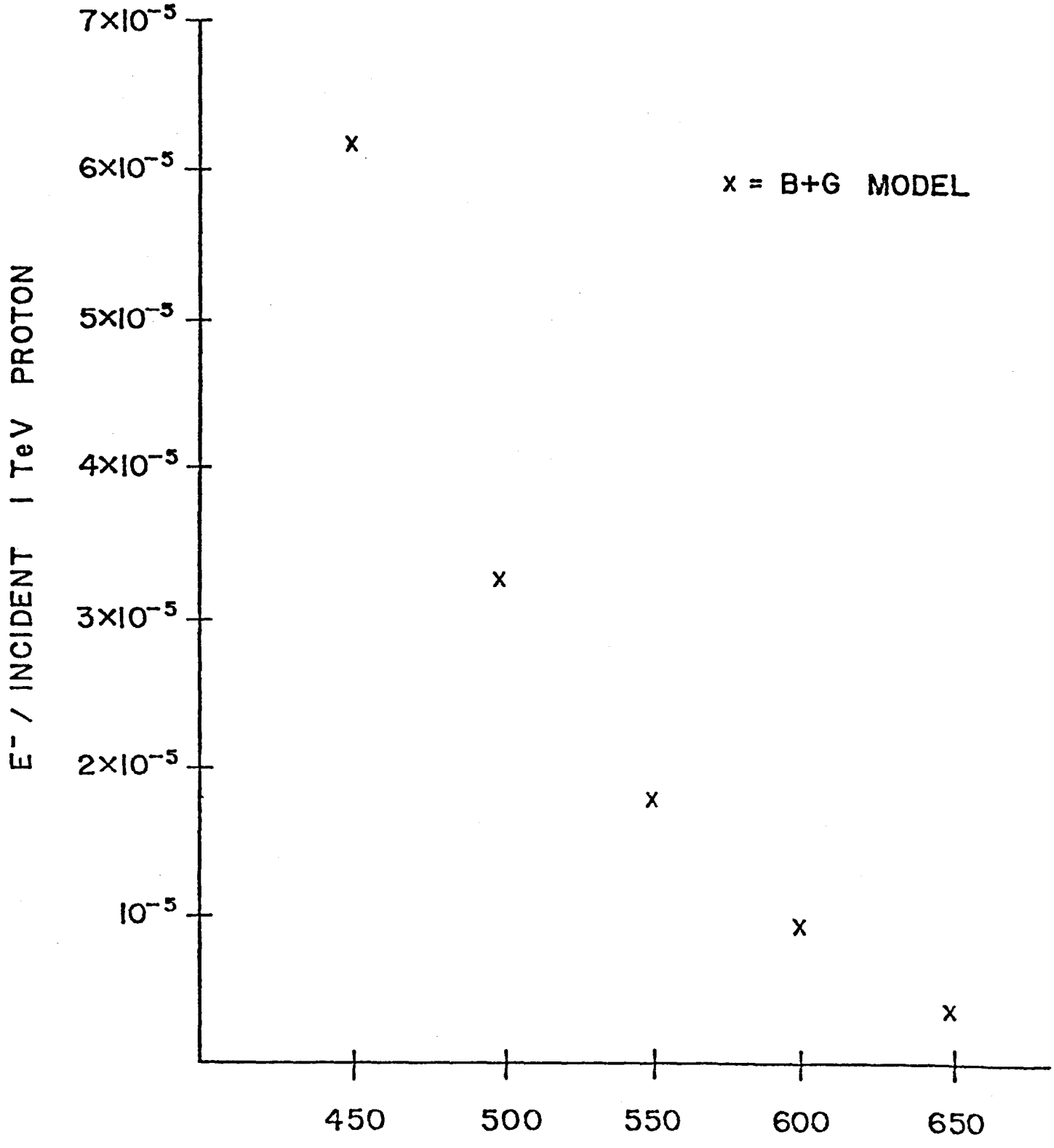
7×10⁻⁵
6×10⁻⁵
5×10⁻⁵
4×10⁻⁵
3×10⁻⁵
2×10⁻⁵
10⁻⁵
E⁻ / INCIDENT 1 TeV PROTON
x = B+G MODEL
450
500
550
600
650
CENTRAL BEAM SETTING (GeV/C)
BROAD BAND BEAM
ELECTRON FLUX

FIGURE 16

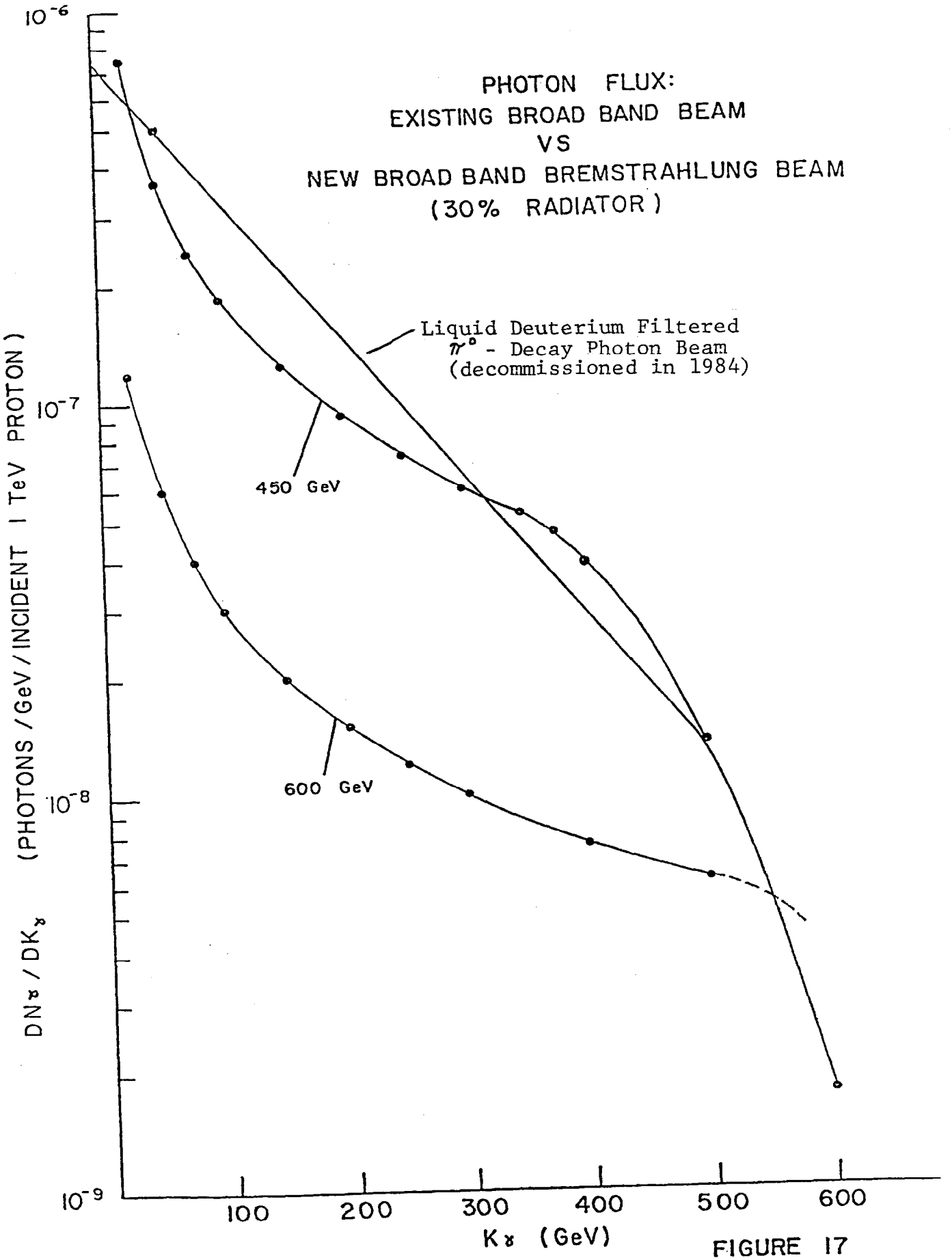
PHOTON FLUX:
EXISTING BROAD BAND BEAM
VS
NEW BROAD BAND BREMSTRAHLUNG BEAM
(30% RADIATOR)
Liquid Deuterium Filtered
π° - Decay Photon Beam
(decommissioned in 1984)
450 GeV
600 GeV
10⁻⁶
10⁻⁷
10⁻⁸
10⁻⁹
DNγ / DKγ (PHOTONS / GeV / INCIDENT 1 TeV PROTON)
100
200
300
400
500
600
Kγ (GeV)

FIGURE 17

FIGURE 18: K^0_L YIELD AND NEUTRON BACKGROUND vs ABSORBER LENGTH

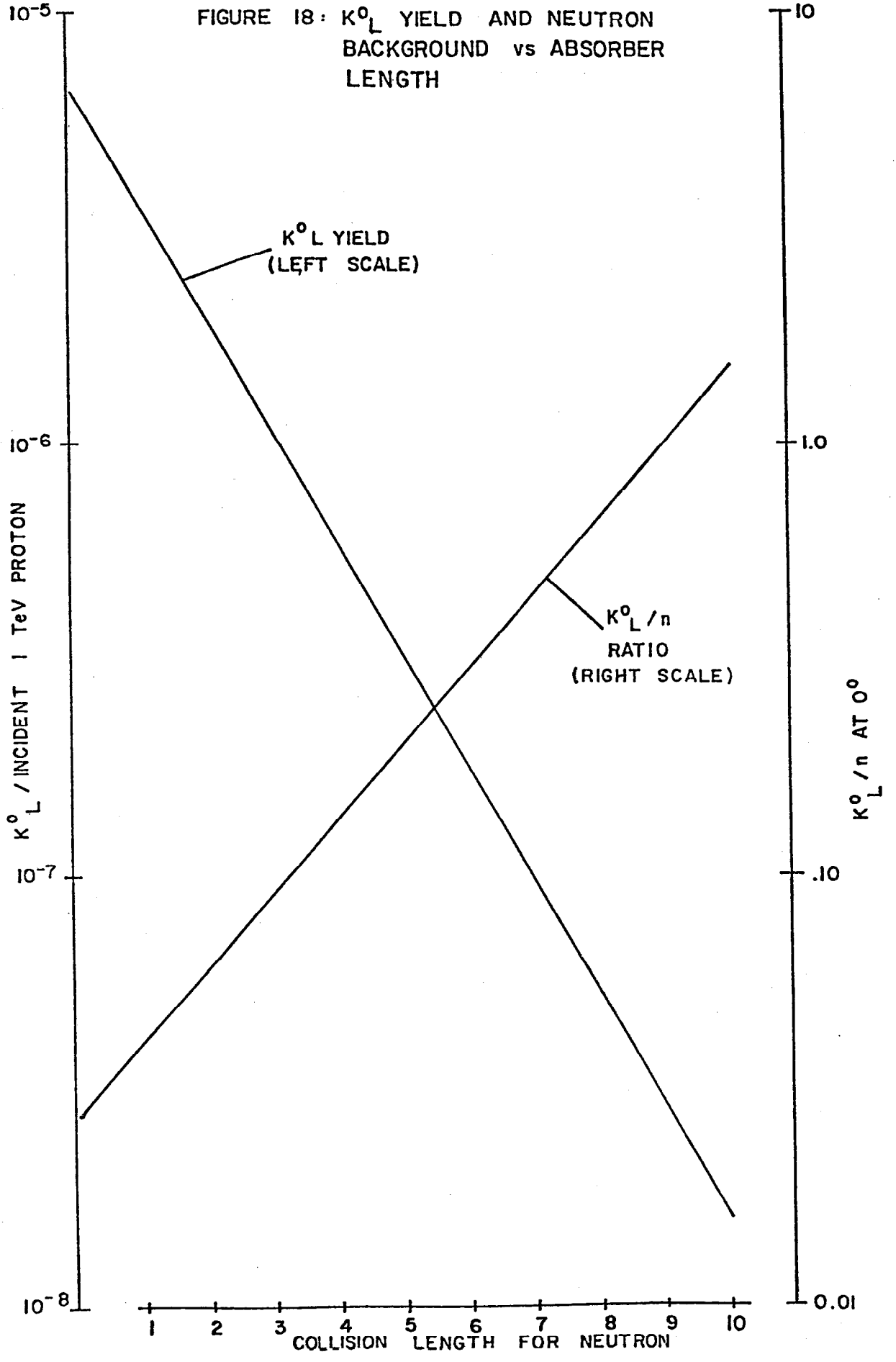

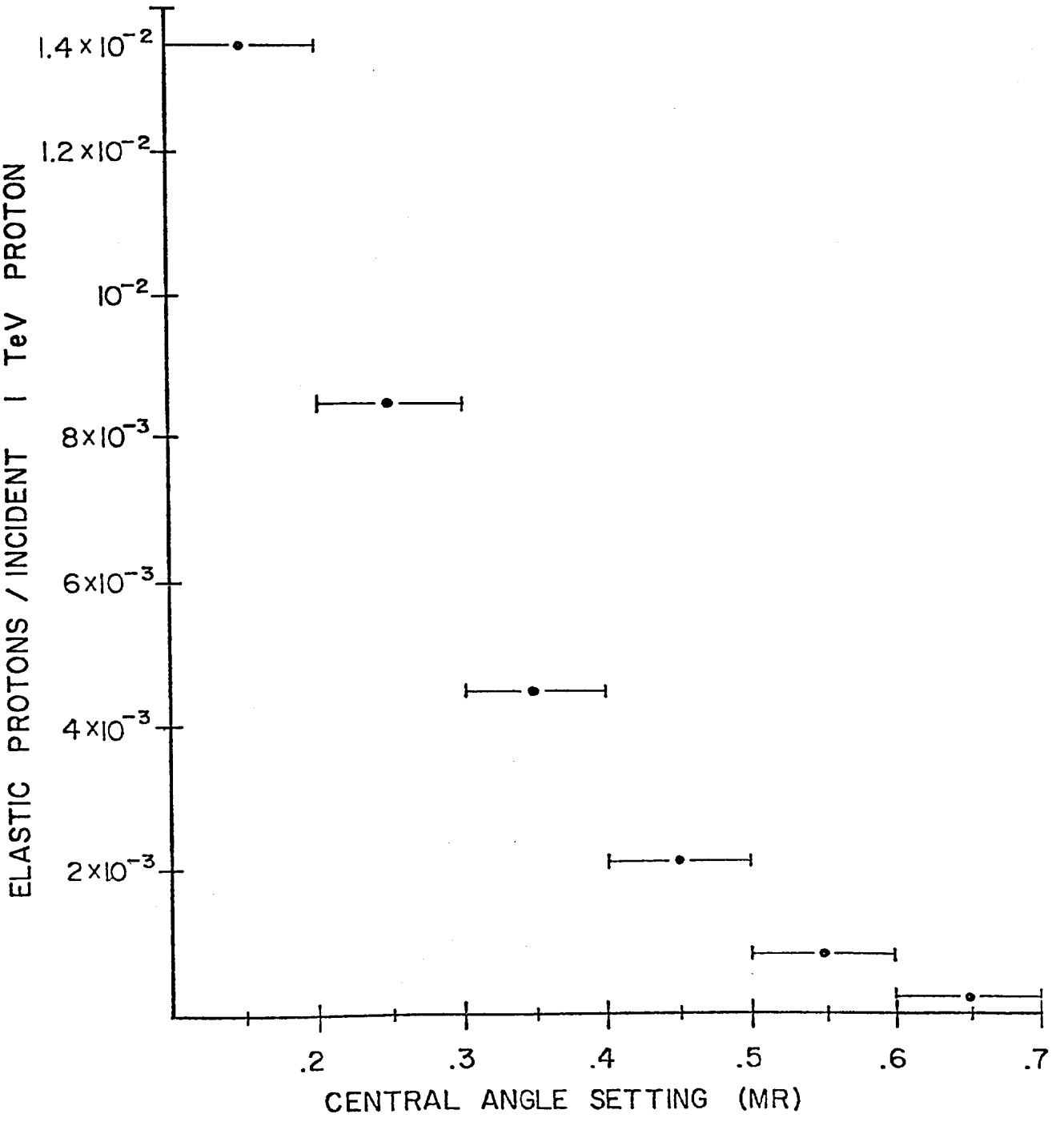
DIFFRACTIVE PROTON BEAM
ELASTIC PROTONS / INCIDENT 1 TeV PROTON
1.4 x 10^-2
1.2 x 10^-2
10^-2
8 x 10^-3
6 x 10^-3
4 x 10^-3
2 x 10^-3
.2
.3
.4
.5
.6
.7
CENTRAL ANGLE SETTING (MR)

FIGURE 19

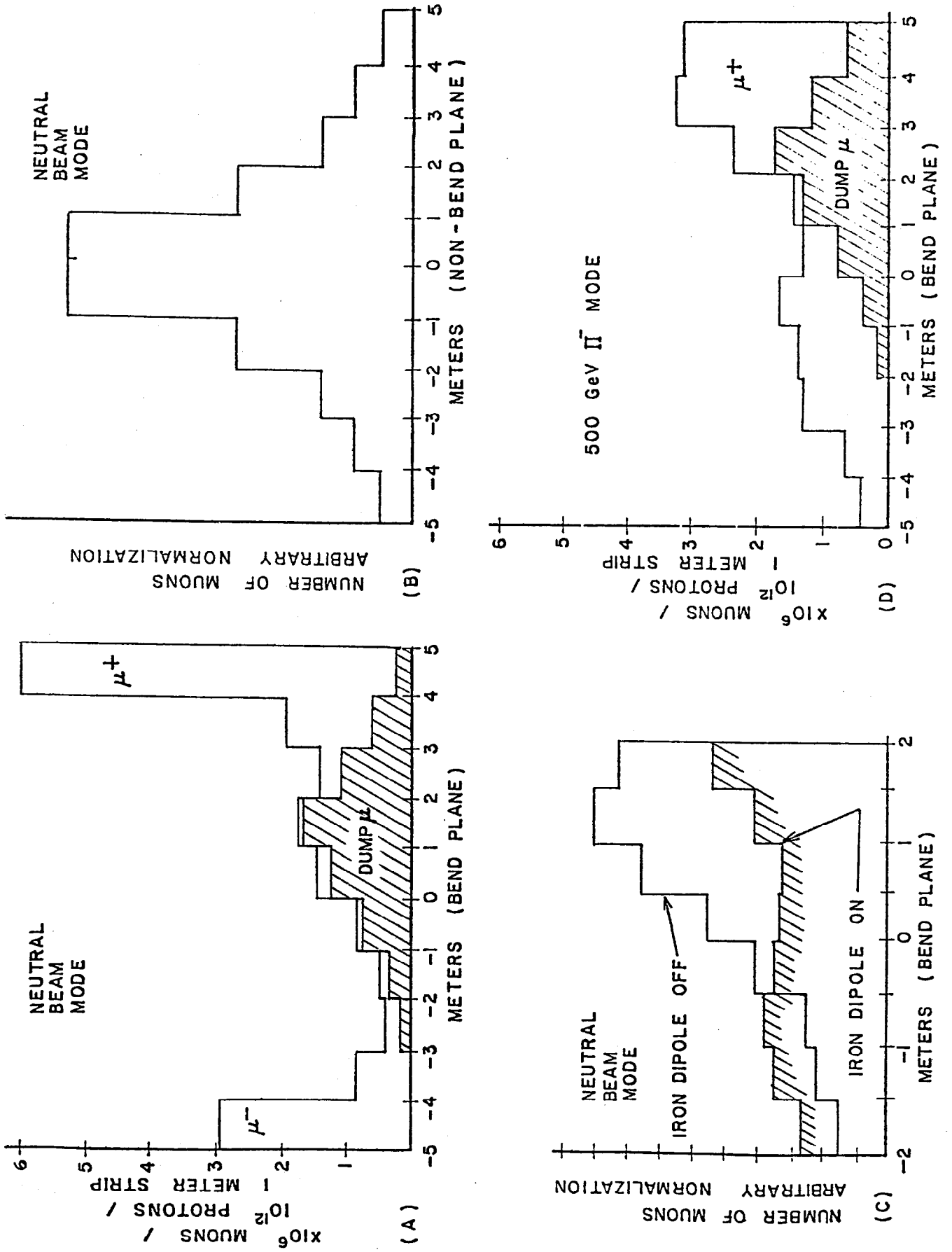
NEUTRAL BEAM MODE
μ^+
μ^-
DUMP μ
METERS (BEND PLANE)
$\times 10^6$ MUONS / 10^{12} PROTONS / 1 METER STRIP
(A)
NEUTRAL BEAM MODE
METERS (NON-BEND PLANE)
NUMBER OF MUONS ARBITRARY NORMALIZATION
(B)
IRON DIPOLE OFF
IRON DIPOLE ON
METERS (BEND PLANE)
NUMBER OF MUONS ARBITRARY NORMALIZATION
(C)
500 GeV Π^- MODE
μ^+
DUMP μ
METERS (BEND PLANE)
$\times 10^6$ MUONS / 10^{12} PROTONS / 1 METER STRIP
(D)

FIGURE 20

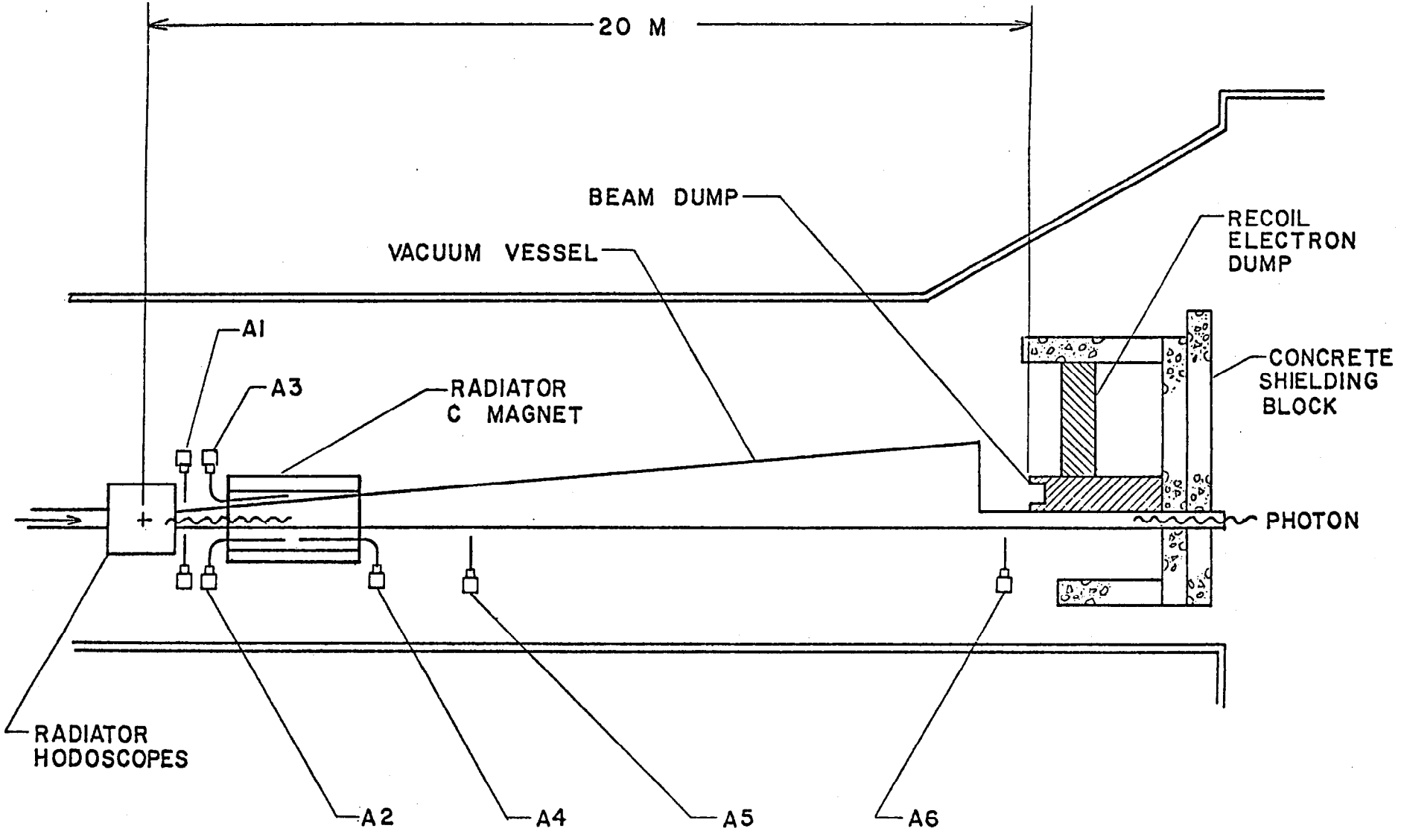
20 M
BEAM DUMP
VACUUM VESSEL
RECOIL
ELECTRON
DUMP
CONCRETE
SHIELDING
BLOCK
A1
A3
RADIATOR
C MAGNET
PHOTON
RADIATOR
HODOSCOPES
A2
A4
A5
A6

FIGURE 21